GRANULAR PESTICIDE DISTRIBUTION PATTERN FROM A HELICOPTER-BORNE SPREADER

BY

MAHESH GHIMIRE

A Thesis

Submitted to the Faculty of Graduate Studies

in Partial Fulfillment of the Requirements

for the Degree of

MASTER OF SCIENCE

Department of Mechanical and Industrial Engineering

University of Manitoba

Winnipeg, Manitoba

THE UNIVERSITY OF MANITOBA

FACULTY OF GRADUATE STUDIES

*****

COPYRIGHT PERMISSION PAGE

GRANULAR PESTICIDE DISTRIBUTION PATTERN FROM A HELICOPTER-BORNE SPREADER

BY

MAHESH GHIMIRE

A Thesis/Practicum submitted to the Faculty of Graduate Studies of The University of Manitoba in partial fulfillment of the requirements of the degree of

MASTER OF SCIENCE

Abstract

A simulation program which could predict the ground deposition pattern of material applied from a air-borne spreader is a prerequisite for developing a control system to vary the flow of the chemical. Deposition pattern could be determined by conducting test in which an air-borne spreader is flown over an array of collectors on the ground and the material collected in each collector is measured. However, the high cost of conducting a field test, and uncertainties involved in such tests justify the simulation study.

A mathematical model is first developed to predict the behavior of a particle ejected from an aircraft. Computer programs are developed to simulate (*i*) particle trajectories and, (*ii*) dry material distribution patterns from a class of helicopter-borne spreader. The aircraft speed, particle size and density, and, the atmospheric wind are found to have significant effect on the deposition uniformity and pattern width. The altitude of the flight is found to have only marginal effect.

Field tests are then conducted to find the actual deposition pattern on the ground and the results are analyzed. Field tests are found to be associated with high degree of uncertainty in terms of variable inputs. Comparison of the experimental patterns with the simulated ones is conducted. The model is found to have potential in predicting the trends in change of deposition pattern shape and size with changes in variables like particle properties, aircraft speed, altitude and wind speed.

Acknowledgements

I express my deep sense of gratitude and appreciation to my thesis advisor Dr. N. Sepehri for his inspiring guidance, valuable suggestions, constructive criticisms and constant encouragement during various stages of the research. My thanks are also due to my thesis committee members Dr. S. Thronton-Trump and Dr. Qiang Zhang for their time to read the thesis.

I wish to acknowledge the financial supports provided by Nepal Engineering Education Project and the City of Winnipeg Insect Control Branch.

I also wish to acknowledge the contributions to the experimental studies of summer research assiatant Heather McKibbin of University of Manitoba, helicopter Pilot Andy Pojer of Western Aerial, Autumn Robbie Draward, and Rob Kubish of City of Winnipeg.

Finally, I would like to dedicate this thesis to my wife Hema and daughter Shreya whose confidence and expectation have been a constant source of support in my career.

Table of Contents

List of Tables

List of Figures

Nomenclature

A = Area, m^2

C_c = coefficient of correlation

C_d = coefficient of drag

C_v = coefficient of variation

D = zero plane displacement, m

D_R = deposition rate, $\frac{kg}{ha}$

d = diameter, m

F = drag force, N

g = acceleration due to gravity, $\frac{m}{s^2}$

h = crop height, m

K = aerodynamic resistance coefficient, $\frac{kg}{m}$

m = mass, kg

Q = mass flow rate, $\frac{kg}{s}$

Re = Reynolds number

S = swath width, m

T = temperature, C

t = time, s

V = velocity, $\frac{m}{s}$

V_G = helicopter speed, $\frac{km}{hr}$

Z = altitude, m

Z_0 = roughness parameter

α = angle with the horizontal plane, *deg*

β = angle with the vertical plane, *deg*

ρ = density, $\frac{kg}{m^3}$

μ = coefficient of dynamic viscosity, $\frac{kg}{m.s}$

Subscripts

a = air

f = fluid

p = particle

t = terminal

x, y, z = components along X, Y and Z directions, respectively

$1, 2, ..$ = locations 1, 2, etc.

Chapter 1

Introduction

1.1 Motivation and Background

Due to a large number of lakes and rivers in Manitoba, high populations of insects, particularly mosquitoes, torment humans annually in the summer months to the point that a need arises for insect control. Every year, City of Winnipeg's Insect Control Branch introduces pesticides into the natural habitat of mosquito larvae, primarily in areas of standing water. Spraying takes place within the city limits, and up to 8 km outside the city's perimeter. The most efficient way to spray pesticides is from the ground, because it allows for a very high degree of control where application rate is concerned. Also, very small areas can be sprayed by individual back-pack sprayer. However, approximately three quarters of pesticide application is accomplished by aerial spraying. This is because the areas of standing water which are the most densely littered with mosquito larvae, are most often either quite large, or extremely awkward and difficult to access by ground.

Aerial application may be carried out using one of the many types and sizes of liquid or granular spreaders, mounted on aircraft or helicopter. Helicopter has the advantage of being more maneuverable and flexible as compared to the aircraft. Granular solid pesticides may be preferred due to the following reasons (Akesson and Yates. 1974):

1. Granular pesticide can penetrate canopy, such as trees and bushes more effectively than the liquid.

2. Drift is less in granular particles.

3. There is no loss of chemical due to evaporation.

A typical helicopter-borne granular applicator system is as shown in Figure 1.1. It is comprised of (see also Figure 1.2) an air blower, two hoppers, a metering device and flow pipes, through which particles leave the system. These components are all connected by a framework to the helicopter. With reference to Figure 1.2, the components of the spreader system are briefly discussed below.

Hopper

The hoppers (component 'C' in Figure 1.2) are large barrel-like containers which hold the granular pesticide. On the helicopter which carries the spreader, there are two hoppers, one on each side, which can both accommodate up to 250 liters of granular pesticide. The actual amount of pesticide that can be safely kept inside the hopper depends on the payload capacity of the Helicopter. Having two hoppers of identical size maintains symmetry and retains equilibrium in aircraft load distribution while the helicopter is in flight.

Size of hopper is a very important factor because it is the major determining factor of how much chemical can be sprayed before returning to the loading pad. It is important to find a balance between the hopper size and load on the helicopter. This is another advantage of granular chemicals over liquid spraying. Because granules are inherently a more concentrated form of the active ingredient, less pesticide by weight is needed to accomplish effective spraying.

Metering Device

The metering device (component 'B' in Figure 1.2) is a small, motor driven auger which is installed at the bottom of the hopper. The auger speed is maintained constant and the flow of the chemical is controlled using a sliding plate which changes the opening of the hopper to the auger (see Figure 1.3).

Blower Assembly

The blower assembly (component 'A' in Figure 1.2) is an encased impeller which produces air flow at a controlled pressure. One blower services the entire dispersal system on both sides of the helicopter. It is located along the centerline of the aircraft, beneath the cab at the front of the helicopter and is connected to the hoppers and the metering devices via flexible tubing.

Outlets

The dispersal tubing is designed with six outlets, three per side, to encourage symmetrical dispersal of pesticide. The amount of chemical flowing through the outlet 'C' in Figure 1.3 can be varied using a screw which moves a deflector plate. The flow stream of the particle is again divided into two parts through the outlets 'A' and 'B' (see Figure 1.3), using a deflector plate. This plate can be adjusted to divert different amount of chemicals by changing its angle, β, with which it cuts the flow stream.

Distribution Pattern

Whatever may be the method of application, the effectiveness of any such application depends upon, (*i*) the correct rate of application and, (*ii*) the evenness of the deposition on the target area. It is common to attain the correct average application rate but have uneven distribution across the treated area (Gardisser, 1992). Hence it

is important to measure the deposition rate and the pattern uniformity to make sure that the target area is getting correct amount of pesticide.

The prevalent practice to determine the uniformity of spread of the applied material is by flying or moving the applicator over rows and columns of collectors on the ground and later collecting the content of each collector and then determining the spread pattern by weighing the content (ASAE, 1982). This method only measures the resulting spread pattern and does not provide any information about how the spread pattern is achieved and what is the contribution of the individual physical properties (Hofstee, 1994).

Studying the effect of individual parameters on the resulting spread and finding the optimum setting for different chemicals and operating conditions by conducting field trials would be time consuming, expensive and impractical in the case of aerial application. The process is an iterative one and since we have no control over some of the important variables like ambient weather condition, it is almost impossible to repeat an experiment in identical conditions. Prevailing weather conditions may prohibit testing or influence the test evaluations enough to make testing during many of the available days impractical. Ideal weather for data collection is usually ideal working weather for aerial applicators, making it difficult for them to participate in data collection activities under ideal conditions (Gardisser 1992).

In view of the above points computer models are being developed to simulate the aerial application of agricultural chemicals (fertilizers, seeds, pesticides). Such models would allow all the best known information to be assembled into a readily available database and evaluated by analysts to make recommendations for adjustments based

on specific information for each application of dry materials. Change in day to day operating parameter may include: material type and characteristics, wind speed and direction, application rate and, aircraft altitude and speed. Quick analysis of specific operating criteria should greatly enhance the chances of making correct adjustments to achieve better application.

Further, due to a growing concern for efficiency in application of farm inputs such as seeds, pesticides and, fertilizers, site-specific management of them is now a major research topic (Olieslagers, 1996). Up to now, field has been treated homogeneously. In site-specific farming it is expected that the required amount of farm inputs varies according to the position in the field. The location of the aircraft relative to the field is determined using a global positioning system (GPS) and the rate of the chemical application is varied according to the field demand map. A control system which could vary the application rate as demand changes is therefore necessary to achieve this. However, to develop a control system, the spreading process needs to be modeled.

1.2 Objective and Scope

The aim of this research is to study and model the deposition of granular pesticide applied from a class of helicopter-borne spreader. The ideal situation would be to have the material broadcasted on the target area at a prescribed rate and have them uniformly distributed across the coverage area. However, most often, this is not achieved. To obtain the settings, that will result in best possible spread, effect of each variable on the deposition pattern must be known. As was discussed earlier, studying the effect of each variable by conducting field tests is not very practical. Computer simulation study is expected to save time and money by giving the user,

ability to analyze various if then scenarios, and arrive at the optimum combination of adjustable variables. To achieve the goal, the following objectives have been set:

1. Model and simulate the particle trajectories, and study the effect of physical properties in the trajectories and spread.

2. Adapt the trajectory model to a class of helicopter-borne spreading system.

3. Conduct experiments on the spreader system during typical flights to determine the deposition patterns.

4. Conduct experiments on the spreader system to determine the flow rates and the effects of meter settings on the flow rates.

The organization of this thesis is as follows. Chapter 2 provides a review of existing literature and theory related to this work. In Chapter 3 the mathematical models are derived. Field tests, which were conducted to determine the actual deposition patterns at various settings, are described in Chapter 4. Also described are the experiments, conducted to study the spreaders capability in accurately metering and delivering the pesticide. Chapter 5 first describes the development of the simulation program; it then presents simulation results, along with comparison with actual field patterns. The thesis is concluded with recommendations and directions for future research in Chapter 6.

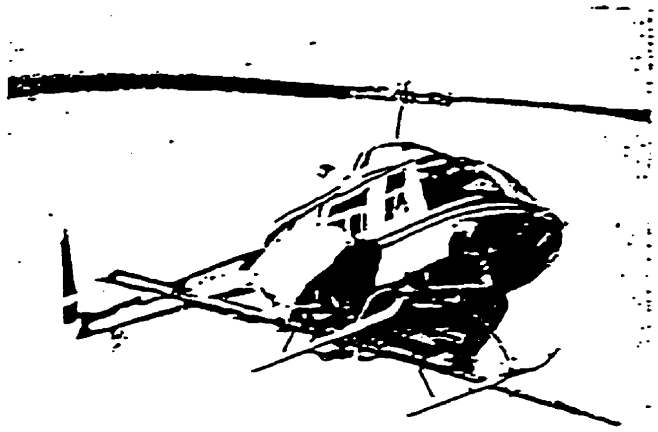

Figure 1.1: Helicopter-borne Spreader.

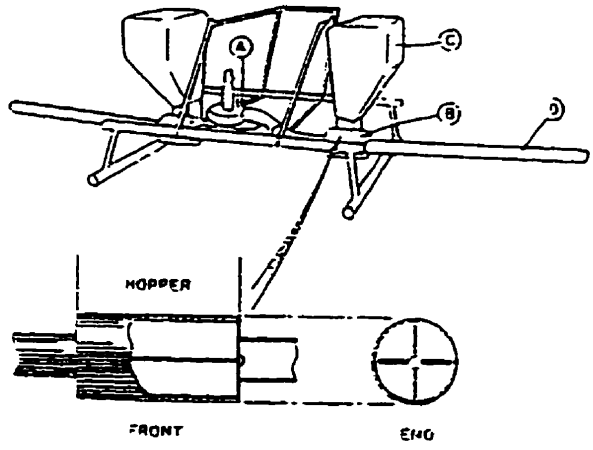

Figure 1.2: Typical Dry Material Spreading System for Helicopter (Akesson and Yates, 1974); (A) Blower,(B) Meter, (C) Hopper and (D) Spreader-Tube.

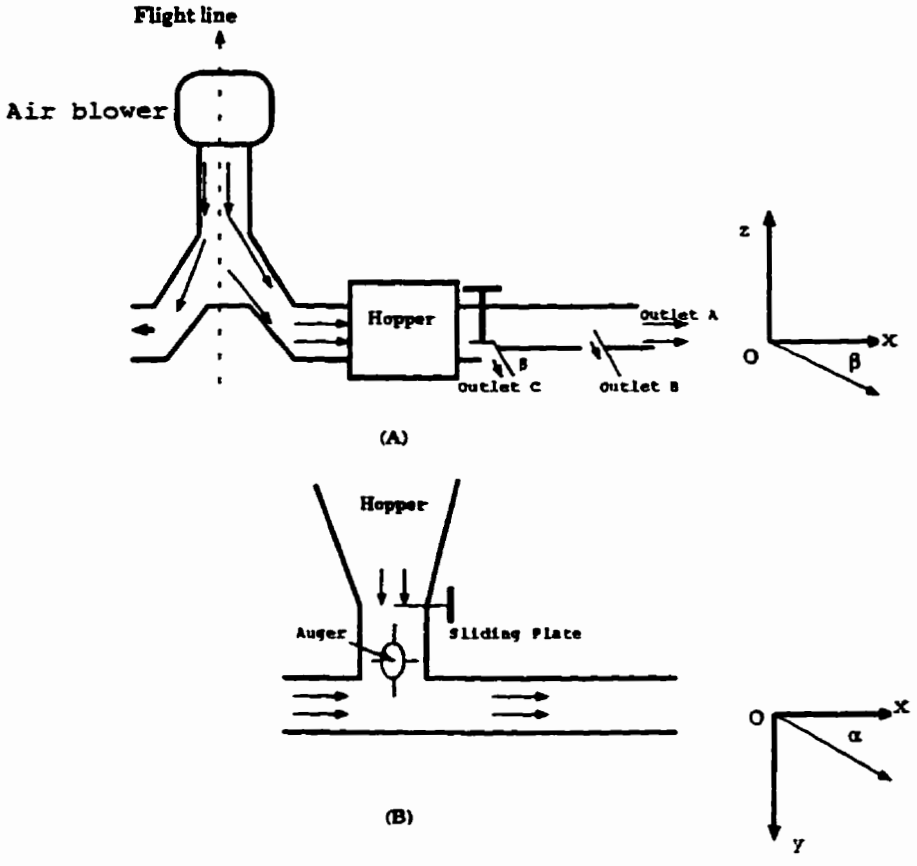

Figure 1.3: Schematic Diagram of a Typical Spreader; (A) Top View and (B) Front View.

Chapter 2

Previous Work and Theory

This chapter provides a survey of previously reported investigations and relevant theories dealing with testing and modeling of ground deposition pattern of chemicals like seeds, granular fertilizers and pesticides. The purpose of this chapter is to identify the state-of-the-art achieved in the areas of field testing, modeling, simulation and, analysis of the distribution patterns from agricultural aircraft. However, focus will be placed on the literature relevant to dry material distribution patterns.

The available literature and theory is classified in two main parts: (*i*) those related to modeling and simulation of particle trajectories and, (*ii*) those related to determination and analysis of distribution patterns.

2.1 Particle Trajectory

Particle motion, from the point where they are metered to the spreader device until they reach the ground, can be divided into (*i*) motion through the air and (*ii*) motion in or on the spreader device. Physical properties of the particle can have different and even opposite effects for both motions (Hofstee, 1994).

2.1.1 Particle Motion Through the Air

Particle motion through the air is independent of the spreader. Only the initial velocity and direction of the particle as it comes out of the spreader is determined by the spreader.

The forces acting on a particle moving through air include, buoyancy force, gravitational force, inertial force and, frictional force. The buoyancy force can be neglected if the density of air (ρ_a) is much smaller than the density of the particle (ρ_p). A set of differential equations, using the balance of the remaining three forces, describe motion of of the particle completely. Real particle trajectories are found to deviate only slightly from the theoretical particle trajectories (Hofstee, 1994). The slight variation may be caused by the eventual tumbling or rotating of the particle.

Reints and Yoerger (1967) derived the following equations to describe two dimensional motion of the particle in air (refer to Figure 2.1) :

$$m_p \frac{d^2x}{dt^2} = -F cos\theta \tag{2.1}$$

$$m_p \frac{d^2y}{dt^2} = -m_p g - F sin\theta \tag{2.2}$$

The drag force, F, is given by:

$$F = \frac{1}{2} C_d \rho_a A_p V_p^2 \tag{2.3}$$

where, V_p is the velocity of the particle, m_p represents mass of the particle. g is the acceleration due to gravity, C_d represents the drag coefficient, ρ_a is the air density, and A_p represents area of particle projected on a plane normal to the direction of

motion.

Coefficient of drag, C_d, is a non dimensional number, value of which depends upon the particle properties and flow condition. Many empirical relations have been suggested by researchers which relate C_d to another non-dimensional number known as Reynolds number, Re. The Reynolds number is given by:

$$Re = \frac{\rho_a V_p d_p}{\mu_a} \tag{2.4}$$

where, d_p is the diameter of the particle, and μ_a is the coefficient of dynamic viscosity of air. μ_a, is a material property and varies with the air temperature. For air, the following relation can be used (Teske, 1993):

$$\mu_a = \frac{0.0076342}{T_a + 296.16}\left(\frac{T_a}{296.16}\right)^{1.5} \tag{2.5}$$

where, T_a is the ambient air temperature.

Figure 2.2 shows how C_d changes with Re. At low Reynolds number ($Re \approx 0.1$), the flow is known as Stokes flow and under these conditions, the coefficient of drag, C_d is given as, $\frac{24}{Re}$. At high Reynolds number($Re \approx 10^3$) the value of C_d becomes approximately constant at about 0.4. When the Reynolds number is within the intermediate range , which is the range of practical interest, the coefficient of drag, C_d varies with Reynolds number in a complicated manner (Morsi and Alexander, 1972).

Reints and Yoerger (1967), fitted an exponential curve and obtained the following equation:

$$C_d = e^{(0.1960 \log Re - 1.885)^{2.377} - 0.9560} \tag{2.6}$$

They solved differential equations (2.1) and (2.2) numerically, using the C_d from equation (2.6). The trajectories for a variety of materials and a number of initial

conditions were determined. The simulated horizontal distances were compared with the experimental observations. It was found that almost all calculated and measured trajectories were within 10% of each other.

The velocity of a particle moving in a fluid changes continuously, until it attains terminal velocity. The Reynolds number, and thus the coefficient of drag depends on the velocity of the particle. Therefore, to calculate the trajectory of a particle moving in a fluid, the instantaneous coefficient of drag must be known. Since no mathematical relationship is available, which would make it possible to calculate it analytically, either an indirect method or an empirical formulae must be derived. Many researchers have formulated empirical relations by fitting an exponential curve to the experimental data points relating C_d to the Reynolds number.

Khan and Richardson (see Haider and Levenspiel, 1989) derived the following relation, after using a nonlinear regression on 300 data points:

$$C_d = (2.25Re^{-0.31} + 0.36Re^{0.06})^{3.45} \tag{2.7}$$

Flemmer and Banks (see Haider and Levenspiel, 1989) proposed:

$$C_d = \frac{24}{Re}10^E \tag{2.8}$$

where,

$$E = 0.261Re^{0.369} - 0.105Re^{0.431} - \frac{0.124}{1+(log_{10}Re)^2}$$

Turton and Levenspiel(see Haider and Levenspiel, 1989), presented the following relation:

$$C_d = \frac{24}{Re}(1 + 0.173Re^{0.657}) + \frac{0.413}{1 + 16300Re^{-1.09}} \tag{2.9}$$

Haider and Levenspiel (1989), suggested the following equation:

$$C_d = \frac{24}{Re}(1 + 0.1806Re^{0.6459}) + \frac{0.4251}{1 + \frac{6880.95}{Re}} \tag{2.10}$$

The goodness of fit, as measured by root mean square (RMS) deviation of these empirical relations are presented in Table 2.1.

For non-spherical particles a non-dimensional number, to account for particle shape, (ϕ) is first defined:

$$Sphericity = (\phi) = \frac{A_s}{A_S}$$

where, A_s is the surface of a sphere having the same volume as the particle and A_S is the actual surface area of the particle. Sphericity, ϕ, gives a measure of how close a particle shape is to the spherical shape. It can be readily calculated that a cube has 0.806 Sphericity and a tetrahedron has 0.607 Sphericity. Haider and Levenspiel (1989) suggested the following relation to calculate the coefficient of drag of non spherical particles:

$$C_d = \frac{24}{Re}(1 + (8.1716e^{-4.0655\phi})) \times Re^{0.0964+0.5566\phi} + \frac{78.69Re(e^{-5.0748\phi})}{Re + 5.378e^{6.2122\phi}} \tag{2.11}$$

The accuracy of equation (2.11) depends upon the Sphericity of the particles. It is reported to vary from 4% to 22% depending upon the particle shape and Sphericity (Haider Levenspiel, 1989). The range of Reynolds number is given as, $Re < 2.5 \times 10^4$.

Table 2.1: Comparison of Fit of Drag Correlations for Spheres

Equations	Range	RMS deviation
(2.7)	$Re < 3 \times 10^5$	0.041
(2.8)	$Re < 8.6 \times 10^4$	0.066
(2.9)	$Re < 2.6 \times 10^5$	0.025
(2.10)	$Re < 2.6 \times 10^5$	0.024

2.1.2 Particle Motion in the Spreader

Kinetic energy is imparted to the particles from the high speed air as they are carried through the tubes or vanes of the spreader. The particle velocity and its initial direction when leaving the spreader has a significant effect on the final location on the ground. Hence it is necessary that particles initial velocity and direction be known in order to mathematically predict where particles will go when they leave the spreader.

Lee and Yates (1977) analyzed the acceleration of an isolated spherical particle in a constant velocity airflow. Considering a particle of mass m_p at rest, being accelerated by air moving at velocity V_a, after time 't' when the particle has traveled a distance 'x' from the rest, the following relation can be written:

$$m_p \frac{dV_p}{dt} = \frac{C_d \rho_a (V_p - V_a)^2 A_p}{2} \tag{2.12}$$

For a spherical particle, m_p is $\rho_p \frac{\pi d_p^3}{6}$ and, A_p is given by $\frac{\pi d_p^2}{4}$. Substituting m_p and A_p in equation (2.12), it is derived that:

$$\frac{3}{4} \frac{C_d \rho_a d_p}{\rho_p} dx = \frac{V_p}{(V_a - V_p)^2} dV_p \tag{2.13}$$

Since the particle starts from rest, $x = 0$ when $t = 0$. Assuming C_d to be constant, the following relation is obtained by integrating equation (2.13):

$$x = \frac{4 \rho_p d_p}{3 \rho_a C_d} (\log(1 - R) + \frac{R}{(1 - R)}) \tag{2.14}$$

where, $R = \frac{V_a}{V_p}$.

Terminal velocity, V_t, of a particle is defined as the constant velocity attained by a particle falling freely in an undisturbed viscous fluid. When a particle is moving at terminal velocity, the gravitational pull is balanced by the drag force on the particle. By equating these two forces the following equation can be derived:

$$V_t = \sqrt{\frac{4 \rho_p d_p g}{3 \rho_a C_d}} \tag{2.15}$$

Substituting V_t from equation (2.15) to equation (2.14), the following is derived:

$$x = \frac{V_t^2}{g}\{\log(1-R) + \frac{R}{(1-R)}\} \tag{2.16}$$

Thus the maximum velocity a particle can attain flowing in a duct depends upon the duct length and the particle terminal velocity, for a given air velocity. Since particle terminal velocity is directly proportional to the square root of the particle size, larger particles attain lower velocity after traveling same duct length than smaller particles. However, due to higher momentum, larger sized particles travel farther than smaller ones, if ejected with the same initial velocity from a spreader exit. Lee and Yates(1977) concluded that there was an optimum range of particle sizes that would give maximum spread. The optimum particles should have terminal velocities of 15 to 20 $\frac{m}{s}$.

Equation (2.16) may be used to determine the particle velocity at the end of a given length of duct. The velocity at the end of the duct is the exit velocity of the particle in the air. Lee and Yates (1977) traced the trajectories of some particles. The actual spread was found to be larger than the range predicted by the model. They attributed this difference to, first, a particle is not alone but surrounded by numerous particles, this may lead to increase in the effective drag in each particle and will tend to increase the early acceleration. The net effect will be a particle exit velocity slightly higher than that calculated. This gives corresponding increase in range for the larger particles. Second, particles are not free from the influence of the air velocity, even after they exit the duct. The exit may act as a nozzle creating a lateral air-jet emerging into a cross flow air-stream. By ignoring this phenomenon, the effective duct length is underestimated leading to corresponding under-assessment of the range of the ejected particle. It was suggested that a larger effective duct length be taken in calculation

to account for the greater spread, so that the range of particle matched with the observed range.

The exit velocity of particles determined by using such a differential equation have limited practical value because mass flows and the interactions between the particles are ignored. Application of these equations to mass flow conditions requires additional knowledge about the interaction between the mass flow and the relevant physical properties. Only very limited information is available about this interaction effect (Hofstee, 1994).

Hofstee (1994) has described a method for measuring the velocity and direction of fertilizer particles discharged by a fertilizer distributor. The technique is based on the Doppler frequency shift of an ultrasonic beam. It is reported that velocity and direction of fertilizer particles could be determined using this technique. This method requires quite elaborate experimental set-up and extensive signal processing.

When a spherical particle travels in a fluid, the particle will generally tend to lag behind the fluid flow (Winoto, 1990). Gardessier (1992) arbitrarily assumed the particle velocity to be 48% of the air velocity in the duct. No basis was provided for using this particular percentage value. Another assumption was that the mean direction of the particles follows the contour of the spreader upon exiting. High speed compact cameras mounted on spreaders to record particle direction during actual application added credence to this theory (Gardessier, 1992).

Particle Flow Pattern in the Spreader

When using air to convey solid particle, the stability of the flow is very important. On decreasing fluid velocity at a constant solid mass flow rate, different flow patterns can be observed. Figure 2.3 illustrates the flow patterns in horizontal pneumatic conveying (Wirth and Molerus, 1985) . At high air velocities the particles are homogeneously distributed throughout the pipe cross-section. This pattern is referred to as fully suspended flow.

Separation of the two phase flow occurs with decreasing fluid velocity. Part of the solid material is carried in the form of strands sliding along the bottom of the pipe as a moving bed while the reminder is conveyed above the sliding strands as a fully suspended flow. If the superficial air velocity is further reduced, the particles will form dunes which are then swept bodily down stream by impinging particles.

At even lower velocities, the particles settle out and form a fixed bed, over which the solid material is carried as a fully suspended flow. Further reduction of air velocity will plug the flow. The last three flow patterns are designated as unstable patterns, which may be dangerous as they tend to choke the system. Therefore in order to ensure a safe operation of an spreader, the knowledge of transition between steady and stable flow and the unstable flow patterns is very important (Wirth and Molerus, 1985).

Critical velocity is defined as the superficial velocity when the flow changes from stable to unstable. The following relation as given by Segler (see Wirth and Molerus, 1985) relates the critical velocity to a combination of only air velocity, V_a, and solids

mass flow rate, Q:

$$V_a = 0.33Q^{0.129} \tag{2.17}$$

The flow rate that can be safely used is thus limited by the type of flow that results. Fully suspended flow must be maintained in the spreader tubes. Unstable flow may cause the plugging and damage the meter. Though safe to operate, the moving bed type of flow pattern is also undesirable. Such flow will cause many particles to slide off the tube in very low lateral velocity and this will adversely affect the uniformity of the deposition pattern and the pattern width.

2.2 Distribution Pattern of Particles

Particle trajectories in and out of the spreader are helpful in determining the impact location of individual particles. However, the effectiveness of any chemical depends upon how uniformly it is spread on the ground. Traditionally the distribution pattern is determined by conducting field tests wherein a spreader applies the chemical while moving over rows and columns of collection surfaces. The amount collected in each collector, when plotted against the location of the surface on the ground gives the distribution pattern. Since this process is very time consuming and expensive, computer simulation is attempted to study the distribution pattern.

2.2.1 Field Testing

Brazelton (1968) described a method for testing distribution patterns from agricultural aircrafts. The method was used to adjust aircraft spreader to obtain as wide swath as possible with a reasonable degree of uniformity. Wide swath are desirable as they enable the pilots to cover more area in same length of flight and time. Brazelton also noted the effect of the air-streams and vortices coming from the propeller wings.

The effect was slight for the large and heavy particles but was more pronounced as the particle size and density decreased.

ASAE Standard (ASAE S386.1, 1988) describes procedures for measuring and reporting application rates and distribution patterns from agricultural aerial application equipment. The Standard recommends that the tests be conducted in calm air or with wind speeds of less than 8 km/hr measured 1 to 3 m above the ground surface or crop canopy. Flights should be made parallel to and within 20 degrees of the direction of the wind to minimize errors due to cross winds. Each part of the test shall be replicated to account for the random variation. A test shall consist of five parts:

1. determination of the output rate from the aircraft,
2. determination of the swath distribution pattern by recovery of the applied materials from suitable target collectors,
3. determination of usable swath width for field applications,
4. determination of rate of application, and
5. determination of uniformity of application.

Bouse (1985), measured the swath patterns for extruded and pressed clay pellets applied from aircraft. A fixed wing aircraft equipped with a venturi type spreader was used for the tests. The aircraft was flown over a flight path perpendicular to a sample collection line consisting of 30, 1 m^2 funnel shaped bins at an ground speed of 168 $\frac{km}{hr}$. The analysis of the date collected showed that:

1. swath width was wider for larger sized particles,
2. cross wind velocity did not significantly affect the total swath width and,

3. cross wind produced lateral shift of the swath patterns. The shift was more for smaller sized particles and was more pronounced if the aircraft altitude was higher.

Whitney (1987), measured the longitudinal and transverse deposition uniformity of aerially applied granular material. Deposition uniformity, as measured by coefficient of variation (C_v), was observed to vary from 14% to 64% percent and from 21% to 67% percent for longitudinal and transverse direction respectively. C_v is defined as the standard deviation times 100 divided by the mean and is a statistical measure of scatter of a set of data relative to the mean.

Spugnoli and Zoli (1989), examined fertilizer spreaders using rotary and pneumatic systems by conducting field tests. The distribution pattern across the swath indicated extreme variability in the operation of the equipment tested. Physical properties of the particles were found to affect the working width of the spreader significantly. Therefore, the authors emphasized the need of providing a detailed explanations of the operations of the spreaders according to the various fertilizers used.

Gardisser (1992), analyzed statistically data obtained from seven years of field tests by various agricultural aviators, to determine which operational variable had the most impact on distribution patterns. The variables studied were, (*i*) wind speed and direction inside the spreader, (*ii*) aircraft and spreader type, (*iii*) aircraft speed and altitude, and (*iv*) material ballistic parameters. All the variables, with the exception of aircraft altitude, were found to have significant effects on the distribution uniformity and pattern width.

2.2.2 Computer Simulation

There have also been many attempts to simulate the particle trajectories in the air and study the resulting deposition pattern on the ground. It was realized early in 1967 that a basic knowledge of trajectories of particles is a prerequisite to designing a broadcast type distributor that will spread a uniform application of seeds or granular fertilizers (Reints and Yoerger, 1967).

Yates et al. (1973) simulated the trajectories of particles dropped from a ram-air spreader mounted on an agricultural aircraft. Equations of motion were solved numerically using a digital computer. The trajectories were traced for different aircraft speed and altitude, particle exit velocity and particle terminal velocity.

Trajectories of particles ejected from aircraft were calculated to assess the effect of: (*i*) angle of ejection relative to flight line (*ii*) forward speed of the aircraft (*iii*) lateral ejection velocity and (*iv*) particle size (Yates et al., 1973). The following equations was used to calculate the drag force, F:

$$F = \frac{1}{2} C_d \rho_a A_p V_p^2 \tag{2.18}$$

When a particle is moving at terminal velocity, the gravitational pull, $m_p g$, to the particle is balanced by the drag force, F. Under free fall conditions, the terminal velocity can be found from:

$$m_p g = F = \frac{1}{2} C_{dt} \rho_a A_p V_t^2 \tag{2.19}$$

where C_{dt} is the coefficient of drag at the terminal velocity.

Thus from equations (2.18) and (2.19), it can be derived that:

$$F = m_p g(\frac{V_p}{V_t})^2 C \tag{2.20}$$

where, $C = \frac{C_d}{C_{dt}}$

Yates et al. (1973) noted that if the particle sizes are large enough and the particle velocity not too small such that the Reynolds number is always in a range where the coefficient of drag remains practically constant, the value of C can be taken as 1. Terminal velocity then gives sufficient description of the particle as far as aerodynamics is concerned. The simulation showed that the spread width (i) increased as the particle terminal velocity increased, (ii) decreased as the forward speed of the aircraft increased and, (iii) increased as the initial particle ejection velocity increased. Yates et al. also verified the theoretical values with experimental results and surmised that they may be a valuable aid in the design of any air-borne distributor.

Simulation models for spread patterns for single impeller rotary distributors were developed (Reed and Wacker, 1970; Davis and Rice, 1974; Ritter et al., 1980; and Pitt et al., 1982). These models calculate the discharge of particles onto a rotating impeller, the motion of the particles on the impeller, the trajectory of the airborne particles and then finds the ground impact point along a line perpendicular to the direction of the distributer travel. In all these models the C_d was taken to be independent of the velocity. These models were developed for spreaders mounted on ground vehicles. Due to the short vertical travel path and fertilizers having relatively larger sizes, no loss of accuracy was expected. It was reported that the swath width could be well predicted and the locations of peaks and valleys could be approximated using this model.

A lot of work has been done to model the travel path of spray materials emanating from aircraft. Teske et al. (1993) reviewed the development of the aerial spray dispersion model FSCBG (Forest Service Cramer, Barry and Grim) developed by the United States Department of Agriculture Forest Service and the US Army. It is reported that this model predicts the behavior of spray materials released through nozzles into the wake of a spray aircraft traveling through idealized atmospheric effects, penetrating a canopy and depositing on the ground. The model includes the spray behavior (evaporation, drift), aircraft wake effects, meteorological influences, canopy interactions, and deposition. It is reported that using this model to dry material distribution is very difficult due to complicated variable inputs (Gardisser, 1992).

Gardisser (1992) developed FERTZ, a PC based computer program to simulate the dry material distribution patterns from agricultural aircraft. This program models Ram-air type spreader applying fertilizer. The following equations of motion in three dimensional space were used:

$$\frac{dV_x}{dt} = \frac{-KV_x\sqrt{V_x^2 + V_y^2 + V_z^2}}{m} \tag{2.21}$$

$$\frac{dV_y}{dt} = g - \frac{KV_y\sqrt{V_x^2 + V_y^2 + V_z^2}}{m} \tag{2.22}$$

$$\frac{dV_z}{dt} = \frac{-KV_z\sqrt{V_x^2 + V_y^2 + V_z^2}}{m} \tag{2.23}$$

where, V_x, V_y, V_z are the velocities in the respective coordinate directions. K is the aerodynamic resistance coefficient and is given by:

$$K = \frac{m_p g}{V_t^2} \tag{2.24}$$

Gardisser (1992) used elutriator to determine terminal velocity experimentally. An

elutriator consists of a vertical tube with a fan. The velocity of the air in the tube is varied within certain range. The velocity of the air that just balances a particle in the tube gives the terminal velocity of the particle (Law and Collier, 1973). The particle was divided into size categories based on sieve sizes and terminal velocity of each size categories were determined using the elutriator.

The effect of atmospheric wind velocity was included in this model from the work of Rosenberg (1984). Under condition of neutral atmospheric stability, the mean wind speed profile over an open, level relatively smooth site can be described as a logarithmic function of elevation. Rosenberg derived the following relation which relates the known velocity at a known altitude to the expected velocity at any altitude:

$$\frac{V_2}{V_1} = \frac{\ln(Z_2 - D) - \ln Z_0}{\ln(Z_1 - D) - \ln Z_0} \tag{2.25}$$

Where, V_1 is the velocity of wind at some known height Z_1 and V_2 is the velocity at height Z_2. D is zero plane displacement and Z_0 is roughness parameter calculated by-

$$\log D = 0.977 \log h - 0.154 \tag{2.26}$$

$$\log Z_0 = 0.997 \log h - 0.883 \tag{2.27}$$

in the above equation, h is the crop height.

Gardisser (1992) concluded that airspeed inside the spreader, cross-wind, aircraft speed, altitude and material flow rate all affected the swath width. Air-speed, aircraft-type, and material flow rate affected the pattern uniformity. As these values increased, swath width and uniformity decreased with the exception of altitude. As altitude increased, swath width increased slightly.

All the simulation models described so far, provide a two dimensional view of the distribution pattern i.e. the expected deposition perpendicular to the line of the motion. Such two dimensional models will be of limited use in developing a control system to vary the application rate so that site-specific deposition rate is achieved. Olieslagers (1996) simulated a spinning disk spreader with the view of developing a control system to achieve site-specific application. To calculate the distribution pattern in the travel direction, the transverse pattern shape and width was assumed to remain constant. The static patterns were elongated and summed, proportional to the travel speed. The sum of these elongated patterns gives the particle distribution in the travel direction.

2.2.3 Pattern Analysis

The final pattern in the field may be quite different from the single pass pattern since there is always overlapping of the succeeding pattern edges to achieve uniform spreading. It may be possible to improve the uniformity of the pattern by overlapping the pattern correctly. But overlapping different amounts will change the average application rate and also very likely change the uniformity.

It is also possible to spread in either of two ways, back and forth across the field or around and around the field. In back and forth application the adjacent swath will be in opposite direction and in racetrack application adjacent swath will be in same direction. If the patterns are not symmetrical about a centerline along the flight, the back and forth spreading will give a much different final pattern than the race-track spreading as shown in Figure 2.4

Reed (1970), developed a computer program that determined the optimum swath

overlap. The program reads the ground deposition data and then overlaps the pattern successively to get a combined pattern that has least coefficient of variation C_V.

Certain pattern shapes like triangular or trapezoidal are more desirable than others since these patterns can be combined to get uniform final deposition. But the distribution patterns are frequently not smooth and regular nor symmetric. Roth et al., (1985), investigated the effect of swath overlapping on some non-symmetrical distribution pattern. Several pattern shapes were selected and evaluated on the basis of varying the swath interval, calculating the coefficient of variation and selecting the largest swath having a minimum coefficient of variation. Three types of non-symmetric patterns, namely, mid-pattern disturbance, pattern-edge disturbance and offset symmetric, were analyzed this way . Both back and forth and race track application method was anysed for each of the non-symmetrical patterns.

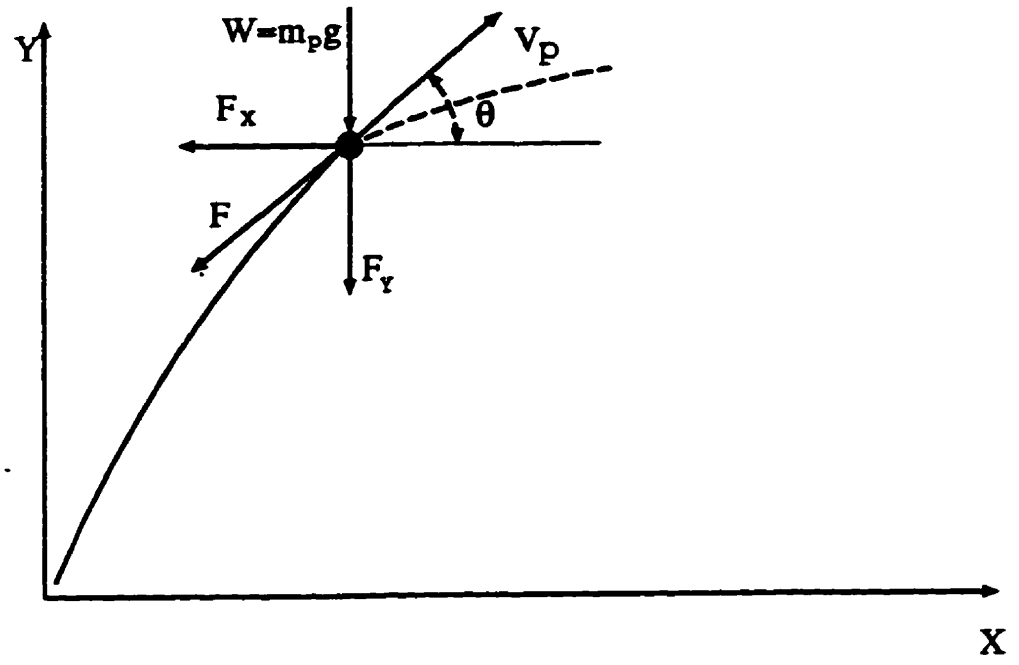

Figure 2.1: Free Body Diagram of Particle in Free flight (Reints and Yoerger, 1967).

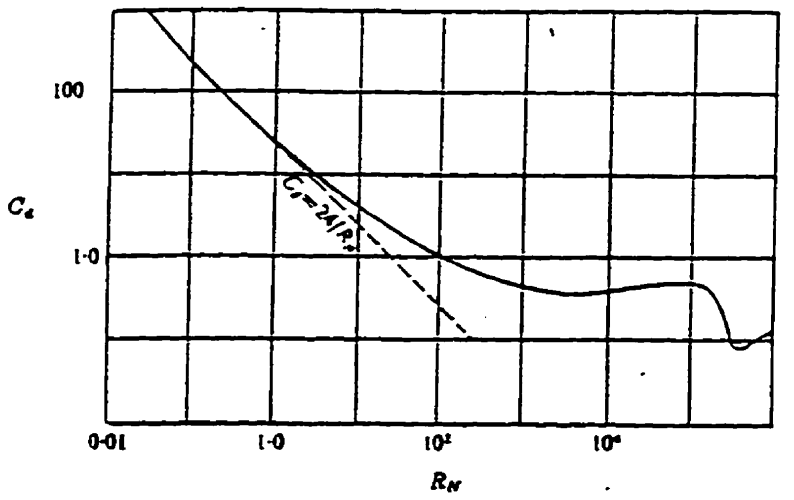

Figure 2.2: Drag Coefficient for Spherical Particles vs. Reynolds Number (Morsi and Alexander, 1972).

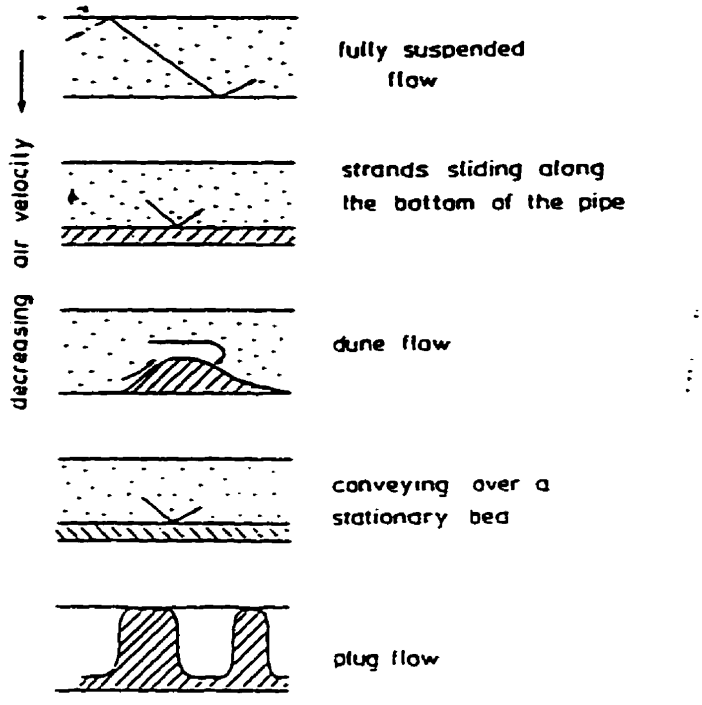

Figure 2.3: Flow Patterns in Horizontal Pneumatic Conveying (Wirth and Molerus, 1985).

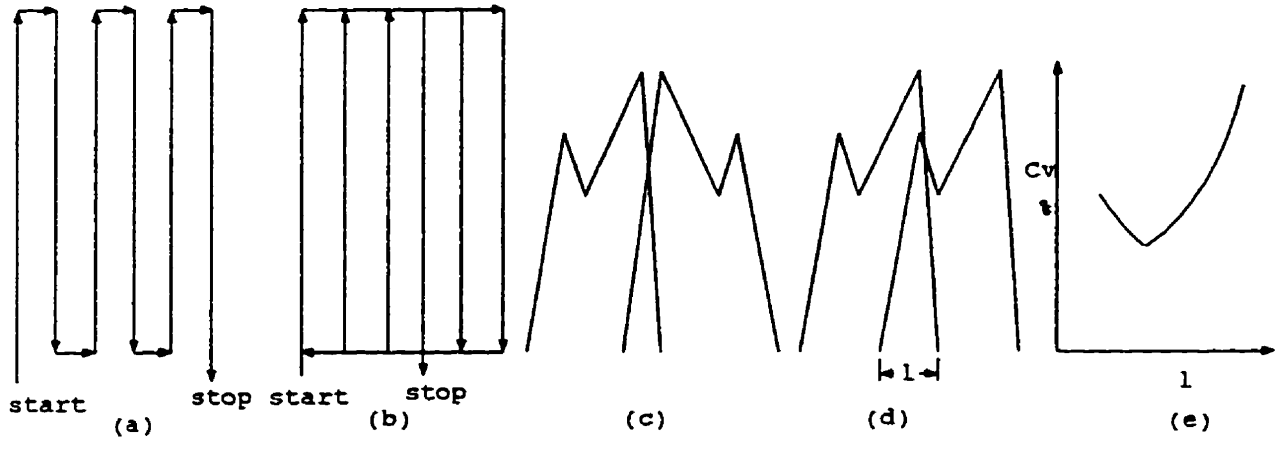

Figure 2.4: (a) Continuous Application, (b) Round-Robin Application, (c) Pattern Overlap in Continuous Application, (d) Pattern Overlap in Round-Robin Application and, (e) Pattern Overlap vs. Coefficient of Variation.

Chapter 3

Model Development

3.1 Particle Trajectory Model

Consider a spreader at an altitude of h. A particle of mass, m_p, diameter, d_p, and, density, ρ_p is ejected from the spreader with an initial velocity, V_{pe}. The final location of the particle on the ground will depend on the initial velocity, direction and the trajectory of the particle. Let α and β be the angle made by the spreader exit with the X axis in XZ and XY planes (refer Figure 3.1) respectively. Assuming that the particle follows the direction of the spreader exit (Gardisser, 1992), the initial particle velocity in three dimensional space can be written as:

$$V_{px} = V_{pe} cos\alpha cos\beta \tag{3.1}$$

$$V_{py} = V_{pe} sin\alpha \tag{3.2}$$

$$V_{pz} = V_{pe} cos\alpha sin\beta \tag{3.3}$$

If the spreader is attached to a aircraft or helicopter which moves along the Z axis with a velocity V_G, then the initial velocity of the particle in Z direction is given by,

$$V_{pz} = V_G + V_{pe} cos\alpha sin\beta \tag{3.4}$$

Once out of the spreader, the trajectory of a particle in the air is determined by the equations of motions arising from the forces acting on the particle moving in air including buoyancy force, gravitational force, inertial force, and drag force. The

buoyancy forces can be neglected because the density of air is much smaller than the density of the particle (Hofstee and Huisman, 1990). Considering the balance of the remaining three forces, the following equations describe the motion of a particle in three dimensional space (refer Figure 3.1).

$$m_p \frac{dV_{px}}{dt} = -F_x \tag{3.5}$$

$$m_p \frac{dV_{py}}{dt} = m_p g - F_y \tag{3.6}$$

$$m_p \frac{dV_{pz}}{dt} = -F_z \tag{3.7}$$

where F_x, F_y and F_z are components of the drag force F. The drag force, F, can be written as: (Yates et al., 1973)

$$F = \frac{1}{2} C_d \rho_a A_p V_{pa}^2 \tag{3.8}$$

where, V_{pa} is the relative velocity of the particle with respect to the surrounding air. This equation can be written in three perpendicular directions X,Y and Z as:

$$F_x = \frac{1}{2} C_d \rho_a A_p V_{pax} \sqrt{V_{pax}^2 + V_{pay}^2 + V_{paz}^2} \tag{3.9}$$

$$F_y = m_p g - \frac{1}{2} C_d \rho_a A_p V_{pay} \sqrt{V_{pax}^2 + V_{pay}^2 + V_{paz}^2} \tag{3.10}$$

$$F_z = \frac{1}{2} C_d \rho_a A_p V_{paz} \sqrt{V_{pax}^2 + V_{pay}^2 + V_{paz}^2} \tag{3.11}$$

Substituting F_x, F_y and F_z from equations (3.9), (3.10) and (3.11) into equations (3.5), (3.6) and (3.7) the following relations can be written:

$$m_p \frac{dV_{px}}{dt} = -\frac{1}{2} C_d \rho_a A_p V_{pax} \sqrt{V_{pax}^2 + V_{pay}^2 + V_{paz}^2} \tag{3.12}$$

$$m_p \frac{dV_{py}}{dt} = m_p g - \frac{1}{2} C_d \rho_a A_p V_{pay} \sqrt{V_{pax}^2 + V_{pay}^2 + V_{paz}^2} \tag{3.13}$$

$$m_p \frac{dV_{pz}}{dt} = -\frac{1}{2} C_d \rho_a A_p V_{paz} \sqrt{V_{pax}^2 + V_{pay}^2 + V_{paz}^2} \tag{3.14}$$

For a spherical particle, $m_p = \rho_p \frac{d_p^3}{6}$ and $A_p = \frac{\pi d_p^2}{4}$. Substituting in equations (3.12) to (3.14) it can be derived that:

$$\frac{dV_{px}}{dt} = -\frac{3}{4}\frac{C_d \rho_a V_{pax}\sqrt{V_{pax}^2 + V_{pay}^2 + V_{paz}^2}}{\rho_p d_p} \tag{3.15}$$

$$\frac{dV_{py}}{dt} = g - \frac{3}{4}\frac{C_d \rho_a V_{pay}\sqrt{V_{pax}^2 + V_{pay}^2 + V_{paz}^2}}{\rho_p d_p} \tag{3.16}$$

$$\frac{dV_{pz}}{dt} = -\frac{3}{4}\frac{C_d \rho_a V_{paz}\sqrt{V_{pax}^2 + V_{pay}^2 + V_{paz}^2}}{\rho_p d_p} \tag{3.17}$$

Equations (3.15) to (3.17) can be solved numerically if the coefficient of drag, C_d is known. As discussed in Chapter 2, the coefficient of drag depends on the particle velocity, and there is no mathematical relation to calculate it analytically. Two different approaches has been employed to solve this problem:

(*i*) Assume that the flow is always in the turbulent region ($Re > 1000$). This enables one to take constant value of C_d of about 0.44 and then solve the equation numerically (Olieslagers et al., 1996).

(*ii*) Experimentally determine the terminal velocity of the particle, V_t, and use it to calculate C_d (Gardisser, 1992).

In first approach, C_d is always taken to be 0.44 irrespective of particle size and velocity. For large and heavy particles and for particles ejected from low altitudes this assumption does not compromise the accuracy. Large and heavy particles are always in turbulent flow regime in air. Small particles which could attain the laminar flow when they travel in their free fall velocity (terminal velocity) impact ground before

this happening in a low altitude ejection. In second approach, C_d is again taken constant, but it corresponds to the particle terminal velocity. Thus particles of different sizes have different C_ds. This approach gives correct value of C_d for the portion of the trajectory in which the particle is moving at terminal velocity.

In this study, C_d is calculated from the current Reynolds number using the following empirical relation developed by Haider and Levenspiel (1989).

$$C_d = \frac{24}{Re}(1 + 0.1806Re^{0.6459}) + \frac{0.4251}{1 + \frac{6880.95}{Re}} \tag{3.18}$$

where, Reynolds number is calculated using the following relation:

$$Re = \frac{\rho_a V_{pa} d_p}{\mu_a} \tag{3.19}$$

Kinetic viscosity of the air, μ_a depends on air temperature and may be calculated using (Teske, 1994):

$$\mu_a = \frac{0.0076342}{T_a + 296.16}(\frac{T_a}{296.16})^{1.5} \tag{3.20}$$

The advantages of this approach are: (*i*) the cumbersome experimental determination of the terminal velocity is avoided and, (*ii*) the model is valid for a wide range of Reynolds number, within which the empirical relation holds. This particular equation has RMS deviation of 0.024 in the range where the Reynolds number is less than 2.6×10^5.

Equations (3.15) to (3.17), have been developed for a single particle flowing in air and may be used in the mass flow condition, providing the concentration of the particles is very low so that the interaction among the particles can be neglected. In the past studies the single particle equations of motion were used to predict the trajectories of particle in air, without any reported loss of accuracy (Yates et al., 1973; Lee and

Yates 1977; and Gardisser, 1992). The reason may be, once out of the spreader device the particles will follow quite distinct trajectories due to the differences in their size, shape and, exit velocity, thus minimizing any effects of their interactions or collisions.

3.2 Deposition Model

The particles inside the spreader are expected to be quite concentrated and the single particle equations, as developed above may not be used. The collision among particles and with the spreader tube walls, the air turbulence, and the rotation of the particles, causes a high degree of uncertainty of any one particle's velocity. Therefore, the modeling of the particle motion inside a spreader is very complex and is out of the scope of the present study. However, it is commonly known that when particles travel in a fluid, the particles will generally tend to lag behind the fluid (Winoto, 1990). Consistent with previous work (Gardisser, 1992) the average velocity of the particles is assumed to be 60% of the air velocity carrying them. The particles are assumed to follow the exit geometry as they emerge from the spreader. From these values of initial velocity and direction the trajectories of the particles are calculated.

Assuming constant density and further assuming that all the particles are spherical, the trajectory of a particle will now depend upon its size only. The size of the material used in aerial application may vary, not only from one material to another but also among particles of the same material. Natural substances like seeds always grow in a range of sizes and manufactured chemical particles too can not be expected to have exactly same sizes due to the unavoidable randomness in the manufacturing processes. Sieve analysis is a commonly used method to separate the continuous size distribution into discrete size groups. Sieve analysis consists of measuring what percentage of

materials is retained in a sieve having standard size of wire mesh. Table 3.1 lists the minimum size a particle can be and be retained on a specific sieve (Gandrud and Haugen, 1985). For example, Referring to Table 3.1, if 50% of a sample of particles is retained in sieve number 18 and out of these 50% are retained in sieve number 20, then 25% of the total particles have size between 1080μm and 925 μm.

Table 3.1: Granular Particle Sizes.

Sieve no.	Maximum opening size (μm)
8	2515
18	1080
20	925
30	660
40	471
60	283
80	207
100	174
170	108
400	48

All the particles in a particular size group are then treated as a single particle of size equal to the mean of the group and the trajectory of such particles are traced using the single particle equations, (3.15) to (3.17). To include the randomness in the particle impact locations it is assumed that particle impacts would also approximate Gaussian distribution (Gardisser, 1992).

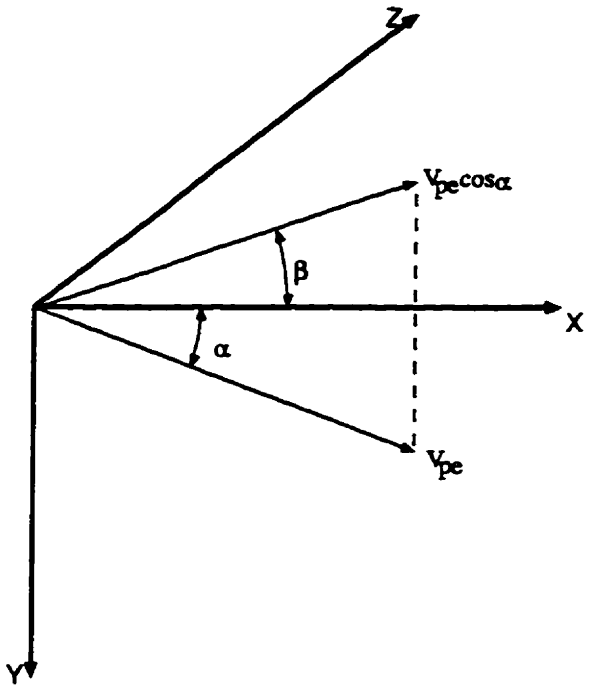

Figure 3.1: Coordinate Axis for the Trajectory Equations.

Chapter 4

Experimental Study

Two types of tests were conducted. In the first set of tests, commonly referred as field test, dry material was applied from an air-borne spreader, and the materials were collected on rows and columns of collectors placed strategically on ground. The amount collected in each collector when plotted against the location gives the deposition pattern.

In the second set of tests the spreader was operated on the ground and its ability in correctly and consistently meeting the flow rate was accessed. The effect of various settings on the flow rate was also measured. These tests are termed as 'stationary tests' henceforth.

4.1 Field Test

It is commonly accepted that distribution uniformity is affected by spreader design, material properties, application rate, aircraft operating parameters and, ambient conditions (Whitney et al., 1987). Field tests are the most popular method of obtaining the deposition rate and the pattern uniformity on the ground.

Field tests were conducted to find the actual distribution on the field. The aim of the field test was to determine the degree of uniformity, both across the flight line

and, along the flight line, which typically exists with current equipment and technology. The tests were conducted by varying the altitude, flight speed, application rate and, spreader setting to study the effect of these variables on the distribution pattern shape and uniformity.

The tests were conducted on mornings of July 1995 and Aug 1996. The wind movement is the least in the mornings due to relatively uniform temperature distribution in the atmosphere. Blanks, provided by the manufacturer of the Dursban (a chemical larvicide), were used to conduct the tests as the actual chemical could be toxic. Blanks undergo the same manufacturing process as the actual chemical, but are void of any active chemical compound.

A field outside the city limit, provided by the Insect Control Branch of city of Winnipeg was selected as the test ground. The layout of the field for distribution pattern is shown in Figure 4.1. Two rows of 21 containers were placed on a line perpendicular to the line of flight and separated by a distance of $1m$, so that a swath of 32 m was obtained on the ground.

The surface cross-sectional area of the collector containers is 0.24 m^2, with dimensions of 40 cm by 60 cm and a depth of 25 cm. The side which is 60 cm long was placed along the axis perpendicular to the line of flight (the swath axis) so that more of the swath was covered by each individual container.

In order to obtain a distribution along the flight line, one row of bins were lined up parallel to the line of the flight at a distance 6.4 m from the flight line, as shown in the Figure 4.1. The bins were kept a distance 5 m apart for a length of 100 m from

the start of the application. The bins were kept 20 m apart for another 100 m. The final 100 m, after the pilot stopped applying was again covered with bins 5 m apart. All the bins were labeled to identify their location on the ground.

The following set of tests were conducted with various altitudes, helicopter speeds, chemical flow rates and spreader settings. Each trial was run twice, yielding two repetition of every test.

Test 1: Standard: Altitude = 50 ft; Airspeed = 80 $\frac{km}{hr}$; Flow rate = 3 $\frac{kg}{min}$.

Test 2: Altitude = 25 ft; Airspeed = 80 $\frac{km}{hr}$; Flow rate = 3 $\frac{kg}{min}$.

Test 3: Altitude = 100 ft; Airspeed = 80 $\frac{km}{hr}$; Flow rate = 3 $\frac{kg}{min}$.

Test 4: Altitude = 50 ft; Airspeed = 70 $\frac{km}{hr}$; Flow rate = 3 $\frac{kg}{min}$.

Test 5: Altitude = 50 ft; Airspeed = 90 $\frac{km}{hr}$; Flow rate = 3 $\frac{kg}{min}$.

Test 6: Altitude = 50 ft; Airspeed = 80 $\frac{km}{hr}$; Flow rate = 6 $\frac{kg}{min}$.

Test 7: Without Dispersal Tube. Dispersal tubes, which directs the flow towards the center of the flight, was removed. Altitude = 50 ft; Airspeed = 80 $\frac{km}{hr}$; Flow rate = 6 $\frac{kg}{min}$.

Test 8: Without Dispersal Tube. Altitude = 50 ft; Airspeed = 80 $\frac{km}{hr}$; Flow rate = 3 $\frac{kg}{min}$.

Test 9: This test was conducted on Aug 1996. The test was simplified viewing the constraint of the resources available. 74 bins were laid side by side in one row perpendicular to the flight, covering the swath of 44.4 m. Helicopter was flown over this row at standard altitude of 50 ft. and speed of 80 $\frac{km}{hr}$. Test was conducted for flow rates of 3 and 6 $\frac{kg}{min}$. In theses tests the dispersal tubes were removed.

4.1.1 Data Collection and Analysis

After each flight the content inside the containers were carefully emptied in plastic bags, using painters soft brush. The content of each bag was weighed to the nearest 0.01 mg, on a digital precision weighing station. The weight of the content of each bag divided by the surface area of the bins(0.24 m^2) gives the deposition rate at the particular location. The deposition rate when plotted against the position of the collectors on the field gives the distribution pattern. Figures 4.2 to 4.10 show the distribution plots.

For statistical comparison, the average deposition rate of each line of collector is calculated. For test 9, only the collectors having non-zero deposition was taken into account, because a strong cross wind swept the pattern and the collector row missed a significant portion of the actual swath.

The pattern uniformity is measured using coefficient of variation, C_v. C_v is defined as:

$$C_v = \frac{Standard\ Deviation}{Mean} \times 100. \tag{4.1}$$

4.1.2 Distribution Pattern Along the Flight

In all the eight tests, with reference to Figures 4.2 to 4.10, the deposition pattern in the flight direction showed a very high application rate at the beginning of the application. It appears that the meter gives a burst of chemical as the application is started and after a short time it resumes operating at normal condition. It is suspected that the granule gets collected at the bottom of the hopper, due to vibration, before pilot starts application and this results in a high deposition at the start of the application. This problem may have serious environmental concern as the high concentration of toxic material may be harmful to not targeted species. Most of the previous researchers have reported results from field tests in which only the transverse patterns were measured. Thus this problem has been undetected/unreported so far.

4.1.3 Distribution Pattern Across the Flight

Test 1

This test was conducted with standard settings. The standard is defined as, helicopter speed of 80 $\frac{km}{hr}$., altitude of 50 $ft.$, and a rate of 3 kg/min. The distribution pattern is as shown in Figure 4.2. Rest of the tests are compared with this test.

Test 2 and Test 3

The altitude of the helicopter was varied for these tests to 25 ft and 100 ft, respectively. As expected a narrower swath for low altitude application and wider swath for the higher altitude application is obtained (Figures 4.3 and 4.4). A higher altitude application also produced a better uniformity of the deposition. The reason being the particles remain longer time in the air, which enables their trajectories to follow diverge paths.

Test 4 and Test 5

The helicopter speed was varied to 70 $\frac{km}{hr}$ and 90 $\frac{km}{hr}$ respectively for these two tests. We expect higher deposition rate when the helicopter speed is decreased and lower deposition rate when it is increased. If the meter maintained a flow rate of 3 $\frac{kg}{min}$, and assuming a swath of 30 m, a speed of 70, 80, and 90 $\frac{km}{hr}$ should result in average deposition of 0.857, 0.75, and 0.666 $\frac{kg}{ha}$ respectively. The tests results however, could not establish such trend (Figures 4.2, 4.5 and 4.6).

Test 6

The flow rate was increased to 6 $\frac{kg}{min}$ for this test. This should result in 1.5 $\frac{kg}{ha}$ over a swath of 30 m. As expected there is an increase of application rate as shown in Figure 4.7.

Test 7 and Test 8

These tests were conducted with the tubes, which are used to direct the particles towards the center of the flight, removed. It was previously reported that the removal of the tubes did not affect the uniformity of the application since the variability in the particle impact location made sure that the center of the swath receives particles (Saunders and Barr, 1992). As can be seen in Figure 4.8 and 4.9 at two different flow rates, the uniformity of the deposition has been affected. Therefore, in our application, the tubes play important role in making sure the center of the pattern receives particles.

Test 9

The result of the field test 96 is plotted in Figure 4.10. As is seen the pattern is swept by the strong cross wind. The pattern shows a increase in deposition rate when the

application rate is increased. The effect of cross wind is very significant.

4.1.4 Summary

A statistical summary of the field tests is given in Table 4.1. In the table the letters P and R denotes helicopter pass and bin row, respectively. For example P1R2 relates to the first pass second row results. In 96 test, since there was only one row, the cells corresponding to second row are left empty. Referring to Table 4.1 and the plots the following are noted:

1. Increase in flow rate (Tests 6 and 7) resulted in increased deposition rate.
2. Higher flow rate resulted in higher C_v values. This means deposition uniformity is worse for higher flow rate.
3. Removal of the belly tube have adverse effect on the pattern uniformity, as shown by the higher value of the C_v (Tests 7 and 8).
4. Flying in lower altitude results in decrease of swath width (Tests 1, 2 and 3).

4.2 Stationary Test

4.2.1 Stationary Test Station

A photograph of the actual spreader is as shown in the Figure 4.11. A test station was developed to conduct tests on the spreader since to conduct tests on the spreader while the helicopter is running was found to be very difficult and unsafe. The hoppers and the spreader tubes are detachable from the Helicopter. A fan driven by electric motor was used to produce the same wind velocity exiting the tube as with the hydraulic blower. The tests were conducted for the Dursban blanks.

Effect of Hopper Level on Flow Rate

This test was designed to access the effect of amount of the chemical inside the hoppers on the output. Ideally the flow rate of the spreader should vary with the rotational speed of the rotor and the opening of the hopper to the auger only. The amount of the chemical coming out of each hopper was collected in plastic bags for a fixed amount of time and the collected amount was weighed. This weight when divided by the time gives the flow rate. Figure 4.12 shows the effect of the material in the hopper to the flow rate. The flow rate is unaffected by the amount of chemical in the hopper.

Effect of Meter opening on Flow Rate

Aim of this test was to observe the effect of the meter opening on the output from the spreader. First the meter was opened to the maximum (refer Figure 1.3). The output rate from each side was determined as before, i.e., collecting the material for a given period in a plastic bags and then weighing the content). This was repeated for decreasing meter opening. Figure 4.13 depicts the change in flow rate with the change in meter opening for each side.

Effect of Deflector settings on the Flow Rate

The stream of material-air mixture is first divided into two parts by a deflector plate that runs vertical along the spreader. Referring to Figure 1.3, the ratio of the amount can be regulated using a screw that pulls or pushes the deflector plate thus changing the area of each partition. It was observed that 20 full turns of the screw moves the plate by 1 *in*. The test was started with the least opening for C and was increased by 4 turns (0.2 *in*) at a time. The change in flow rate from each outlet as the deflector

position is changed is shown in Figure 4.14.

Referring to Figure 1.3 the rest of the stream is again divided into two parts with the help of a deflector plate "B". The angle of the deflector plate can be varied. At 0 degree the plate is parallel to the spreader pipe and all the stream is directed towards the outlet A. As we gradually increase the angle, more and more of the stream is directed towards B. Readings were taken for various angles of the deflector plate. The effect of the deflector plate angle on the flow rate from exits A and B is as shown in Figure 4.15.

4.2.2 Summary

As was discussed in Section 4.1, the field test showed a very high output from the spreader at the beginning of the application. No such phenomenon was observed when the tests were conducted on the ground. Therefore the bursting of the material at the start may be associated with the vibration of the metering device when attached with the helicopter.

The patterns across the flight showed that the deposition patterns were far from being uniform. Above 60% Coefficient of Variation values were typical. The patterns were not symmetric to the pattern centerline. The average deposition rates were significantly different for two flights of the same test (refer Table 4.1). The flow meter was not able to maintain a consistent flow rate. The shape of the patterns were also significantly different from one flight to another and thus making it impossible to draw any conclusion about effect of operating conditions and material properties on the pattern shape.

The spreader may have been designed for a higher flow rate. The calibration curve of Figure 4.13 shows that the region near 1 $\frac{kg}{min}$ is nonlinear. Since the spreader was used to maintain a flow rate at this region, setting of the meter in this region was very difficult. It was observed that the operator had to undertake quite a few trials to maintain an approximate flow rate. The flow rate was adjusted using a sliding plate at the bottom of the hopper. Using this mechanism, it was very difficult to change the flow rate by 0.2 or 0.5 $\frac{kg}{min}$. Even a small movement of the sliding plate changed quite large area of the opening. Thus, the metering system may not be suitable for the low application rate under the study. It was also observed that the amount of material in the hopper had no effect on the flow rate for the range (15 to 75 kg) tested as seen in Figure 4.12. The deflector plates in the spreader tube were effective in changing the amount of materials going through each outlet as seen in Figures 4.14 and 4.15.

Table 1:

Tests	Average (*kg/ha*)					Coeff. of Variation (%)				
	P1R1	P1R2	P2R1	P2R2	Avg..	P1R1	P1R2	P2R1	P2R2	Avg.
Year 95										
1	0.28	0.3	0.73	0.86	0.54	57	88	142	161	112
2	0.51	0.79	0.59	0.64	0.63	82	120	102	107	103
3	0.95	0.9	0.65	0.64	0.79	61	73	58	53	61
4	0.54	0.6	0.73	0.87	0.69	63	87	37	57	61
5	0.66	0.6	0.73	0.65	0.66	97	93	85	78	88
6	1.06	1.0	0.79	0.81	0.92	161	137	141	150	147
7	1.5	1.49	1.02	0.93	1.24	268	263	143	117	198
8	1.24	1.31	0.76	0.76	1.02	142	132	90	87	113
Year 96										
9 (a)	0.51		0.6		0.56	50		31		41
9 (b)	0.96		1.17		1.07	30		67		49

Table 4.1: Summary of Field Tests.

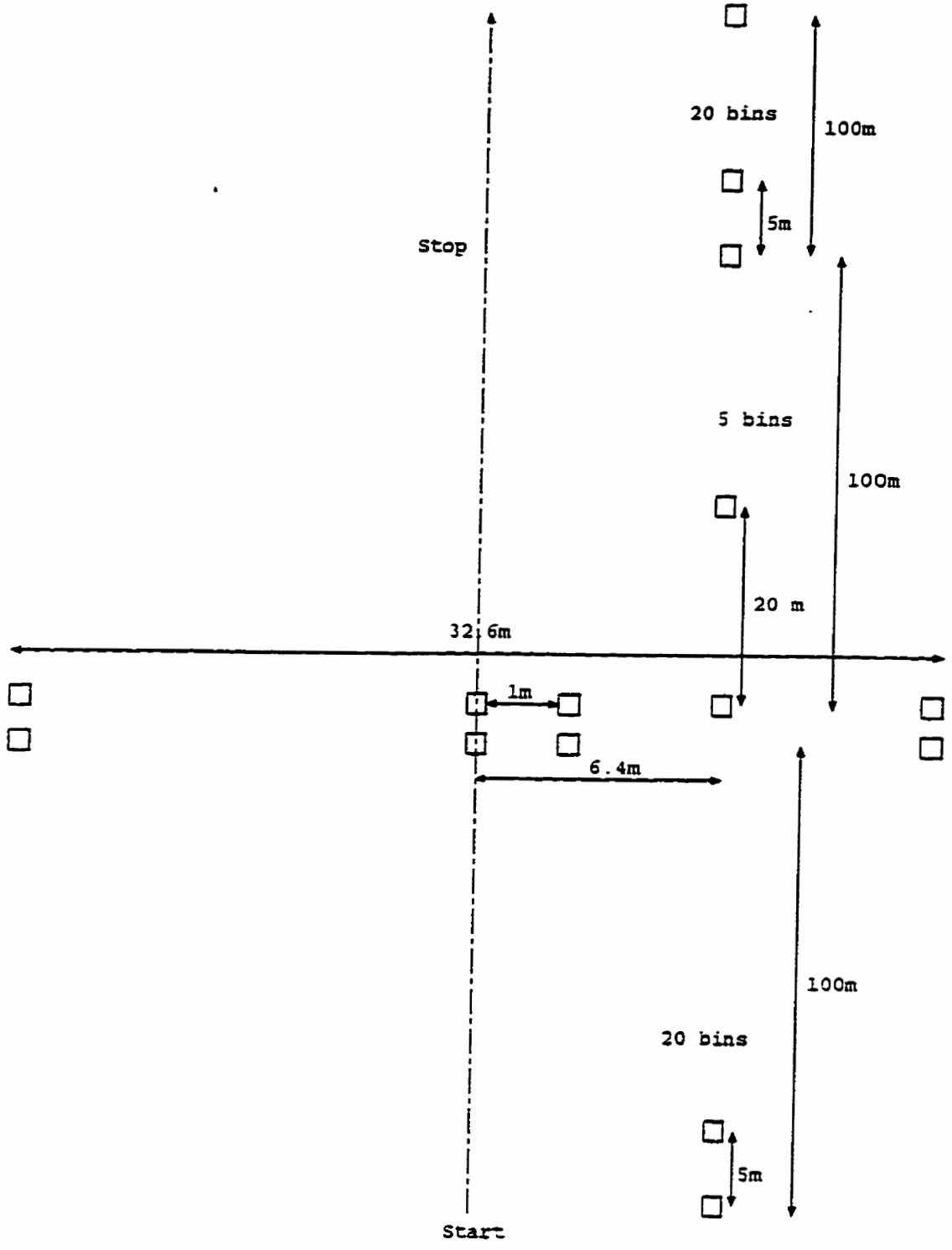

Figure 4.1: Field Lay-out for Tests 1-8.

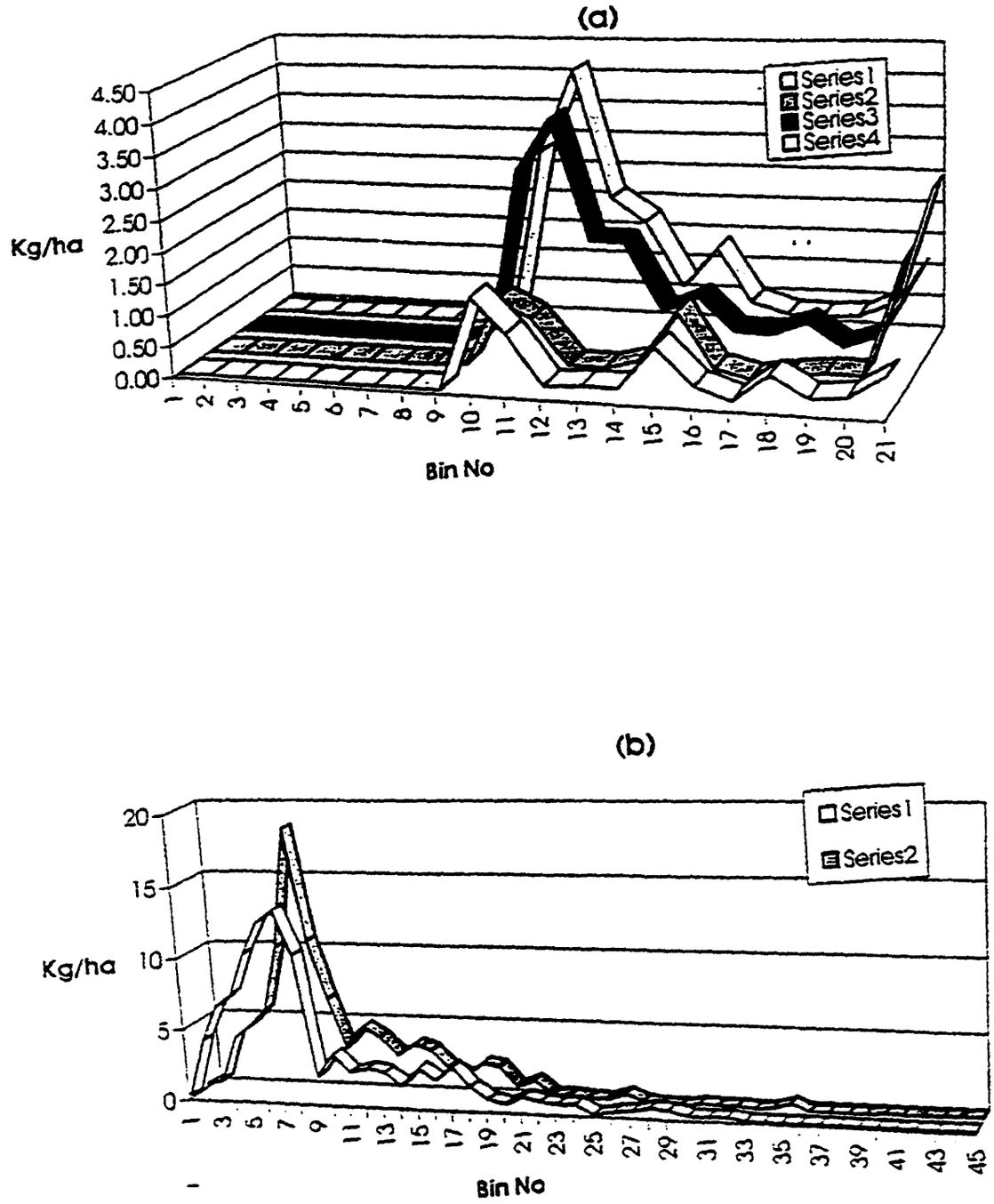

Figure 4.2: Test 1: (*a*) Pattern Across the Swath: (*b*) Pattern Along the Swath.

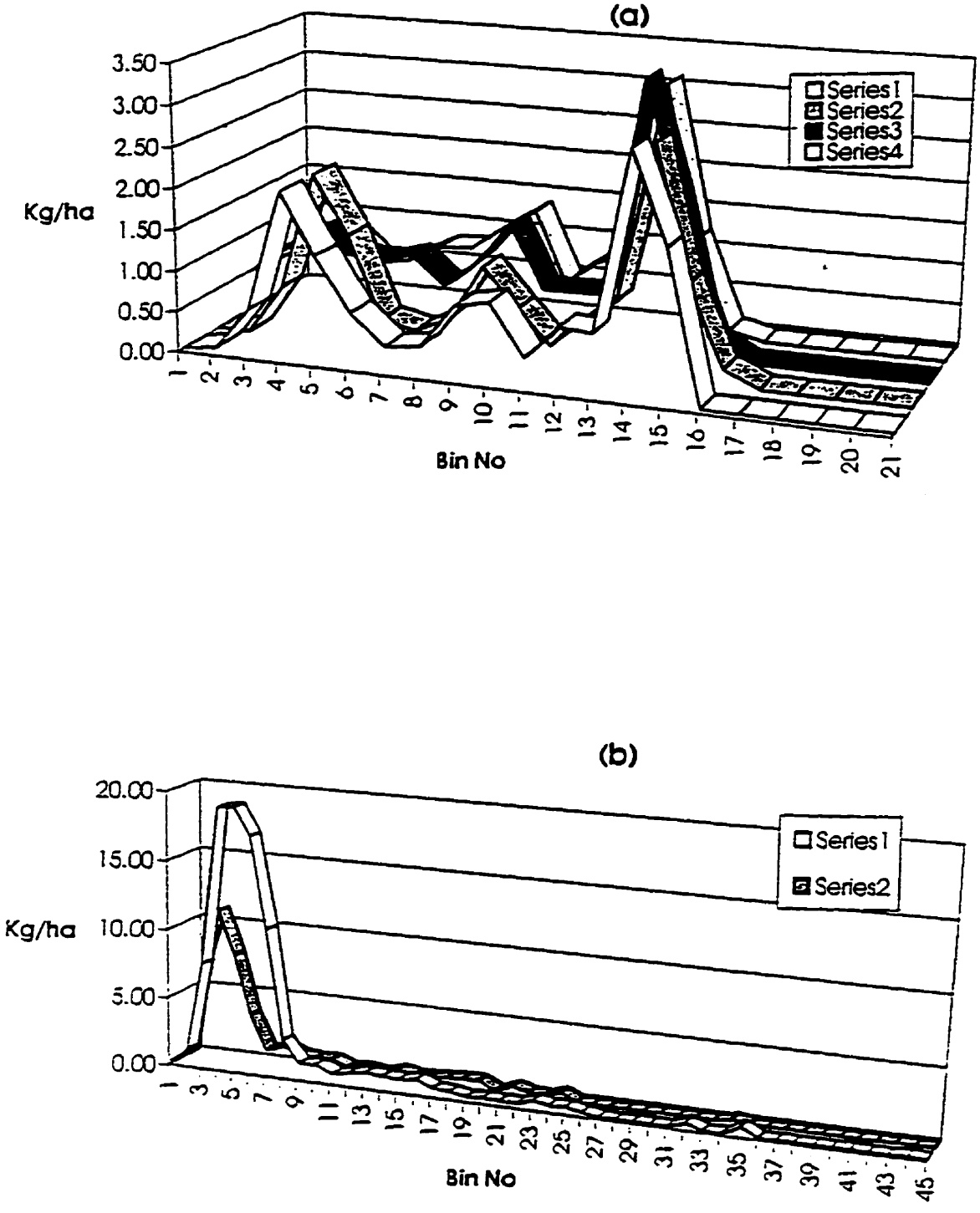

Figure 4.3: Test 2: (*a*) Pattern Across the Swath: (*b*) Pattern Along the Swath.

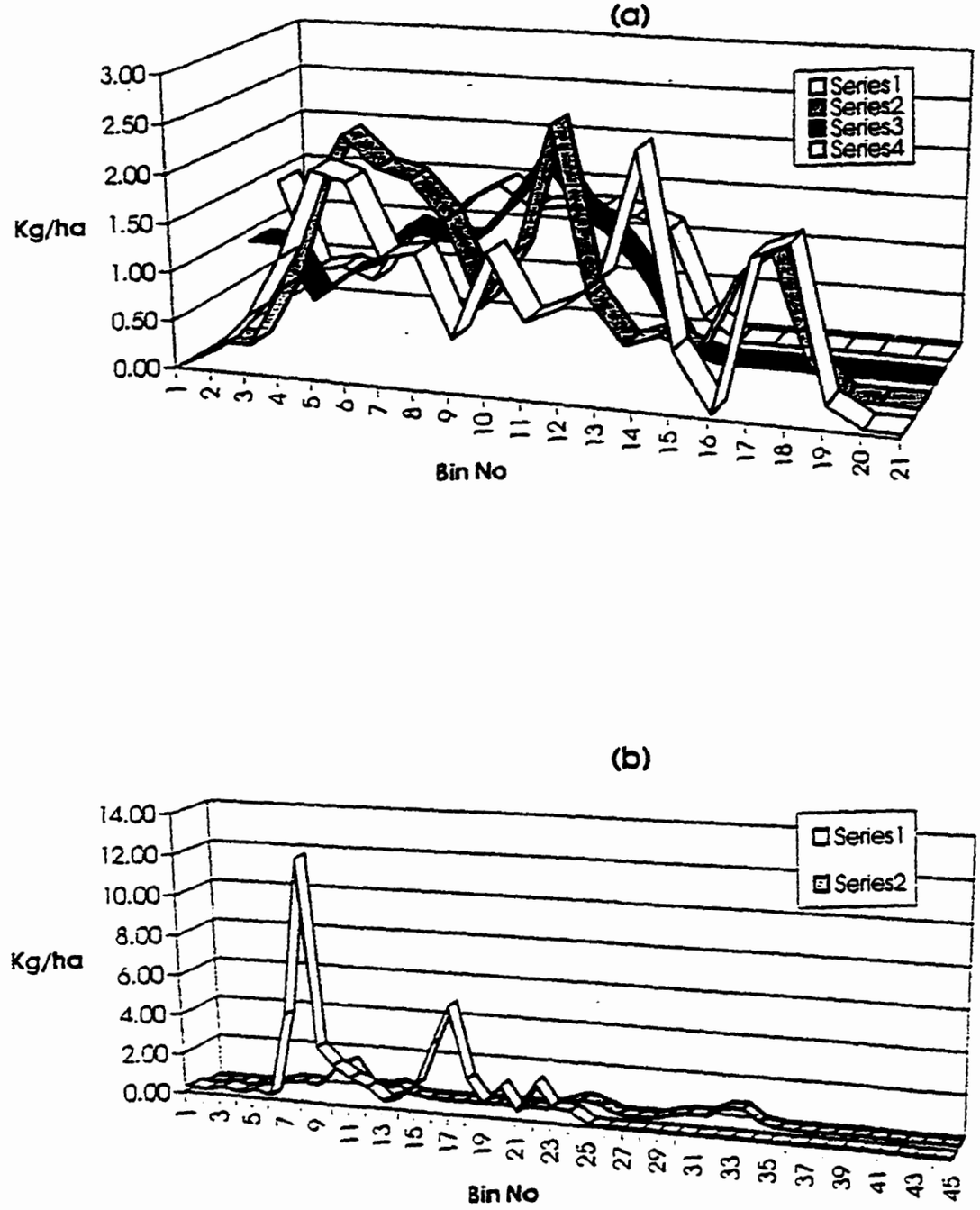

Figure 4.4: Test 3: (*a*) Pattern Across the Swath: (*b*) Pattern Along the Swath.

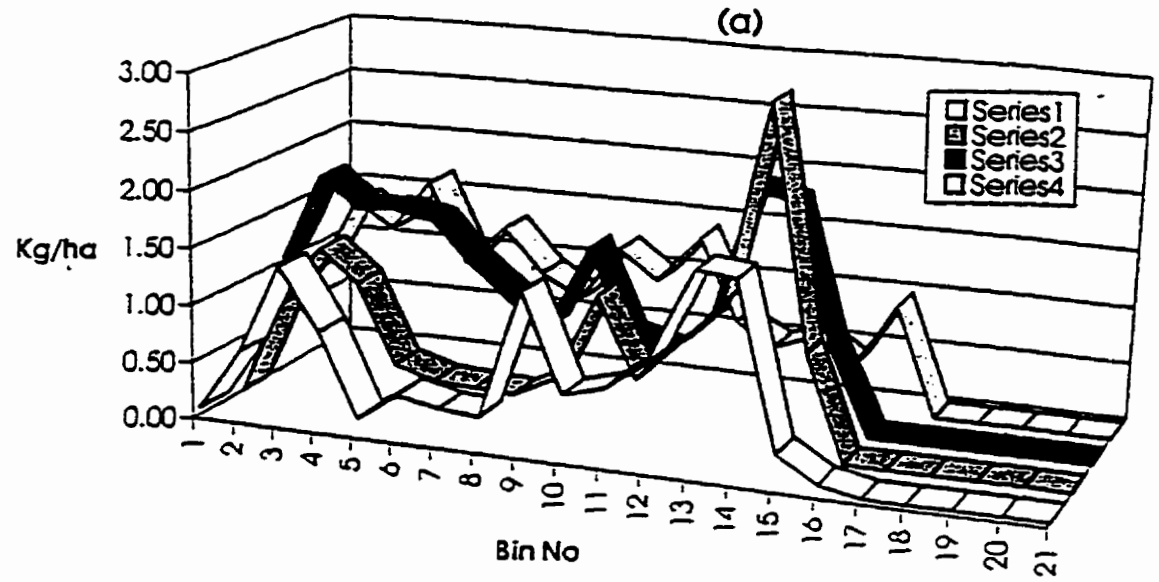

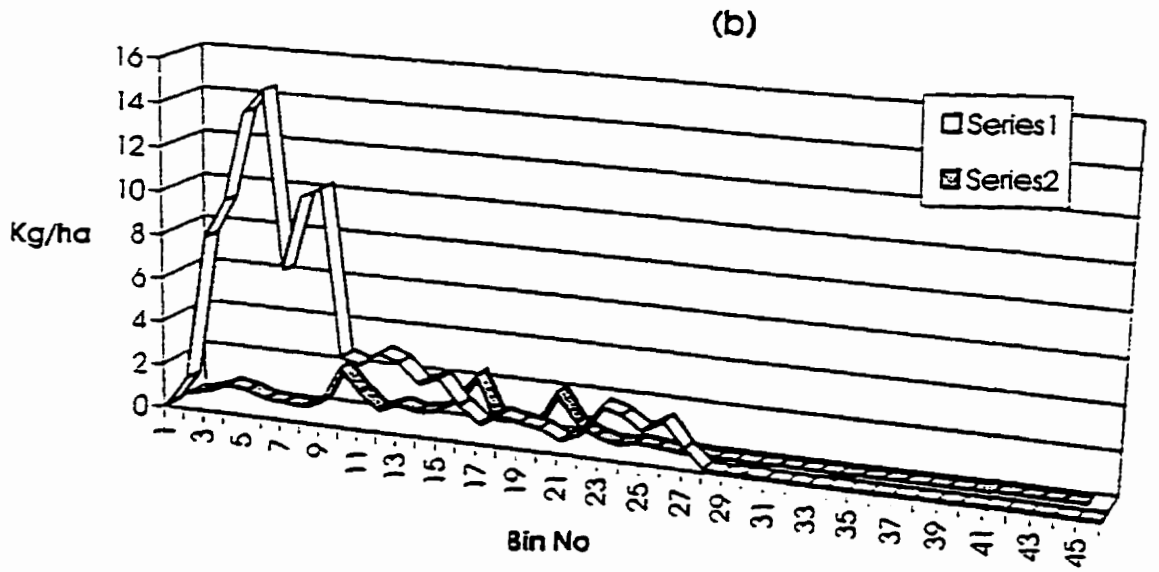

Figure 4.5: Test 4: (*a*) Pattern Across the Swath: (*b*) Pattern Along the Swath.

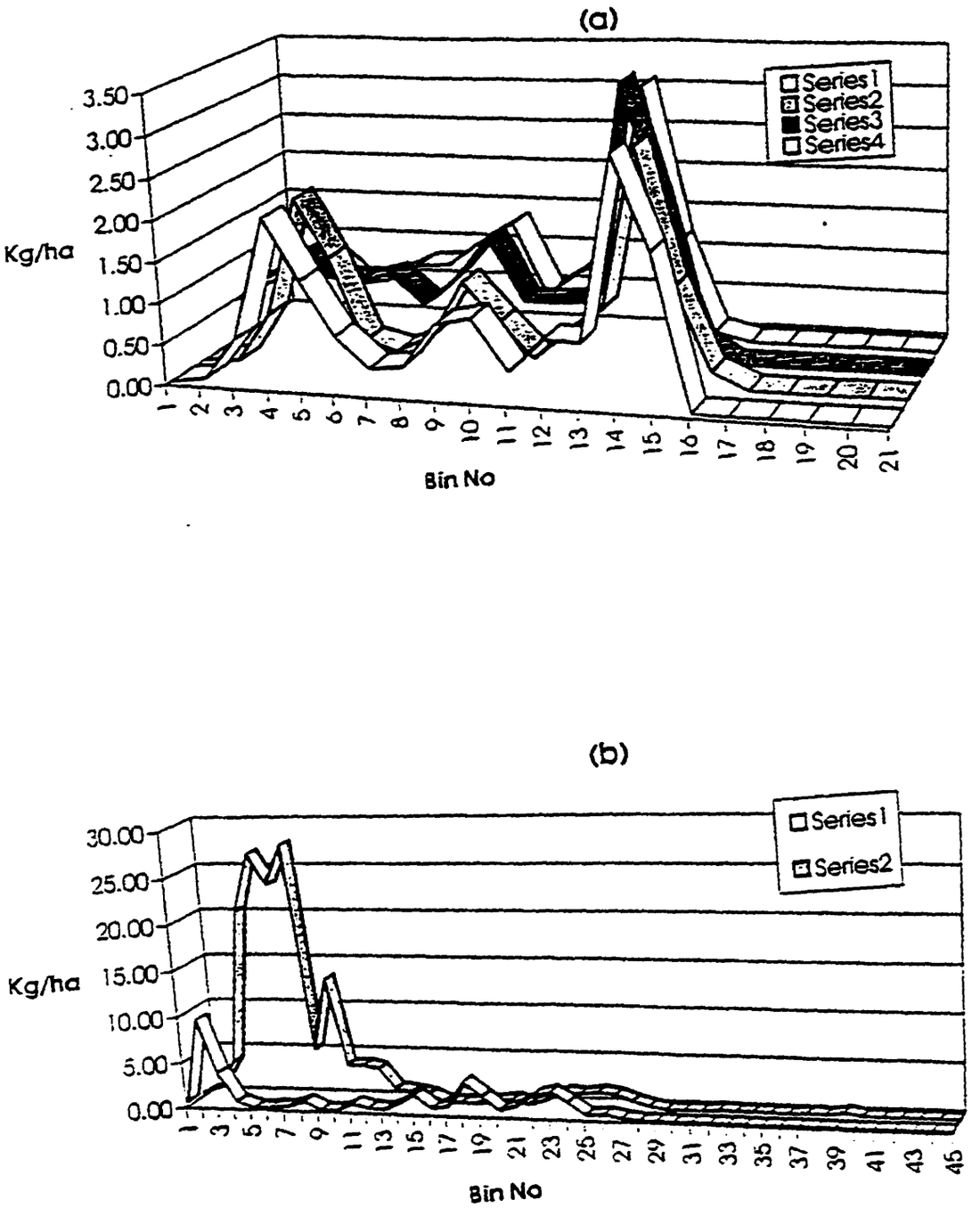

Figure 4.6: Test 5: (*a*) Pattern Across the Swath: (*b*) Pattern Along the Swath.

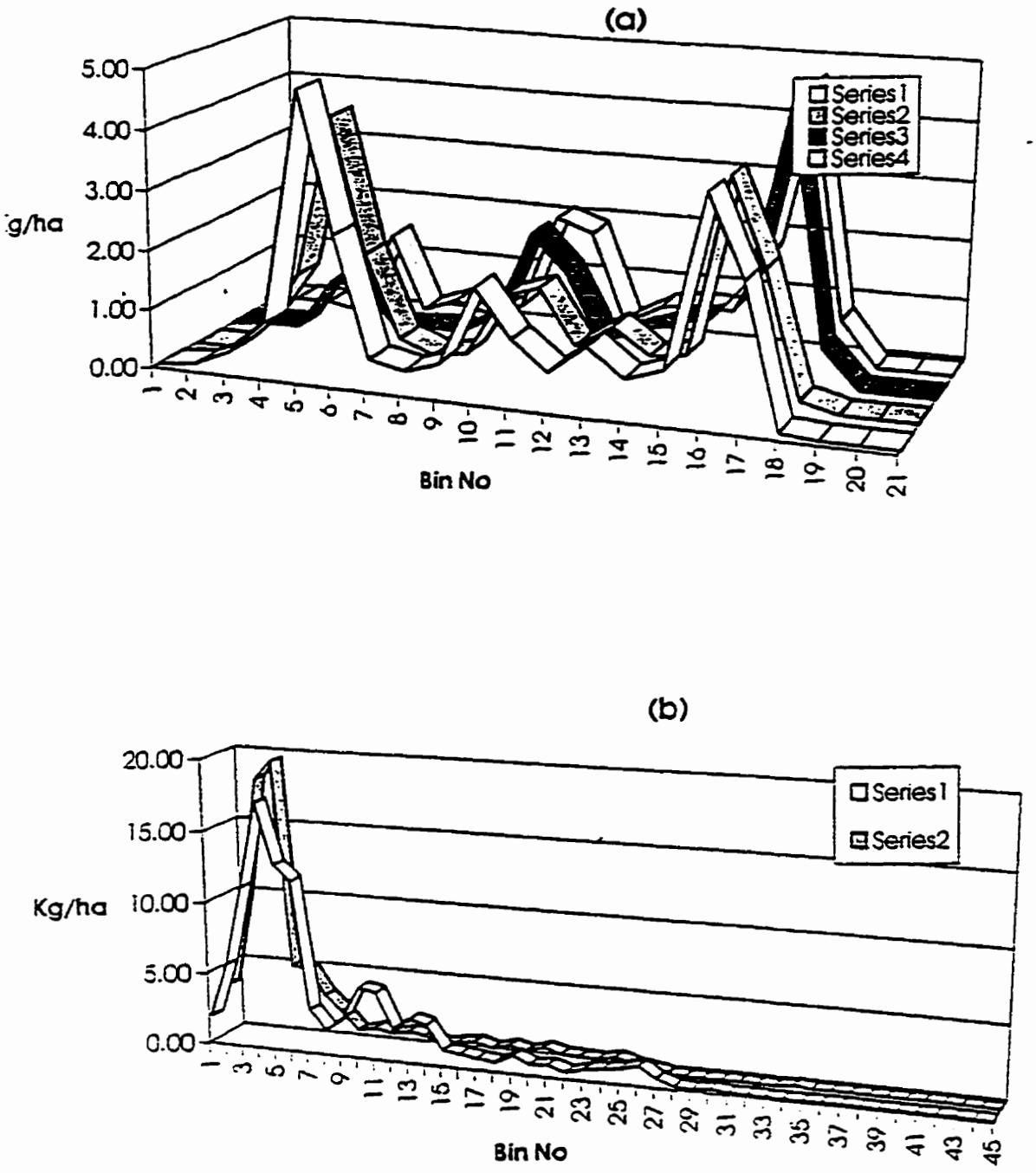

Figure 4.7: Test 6: (*a*) Pattern Across the Swath: (*b*) Pattern Along the Swath.

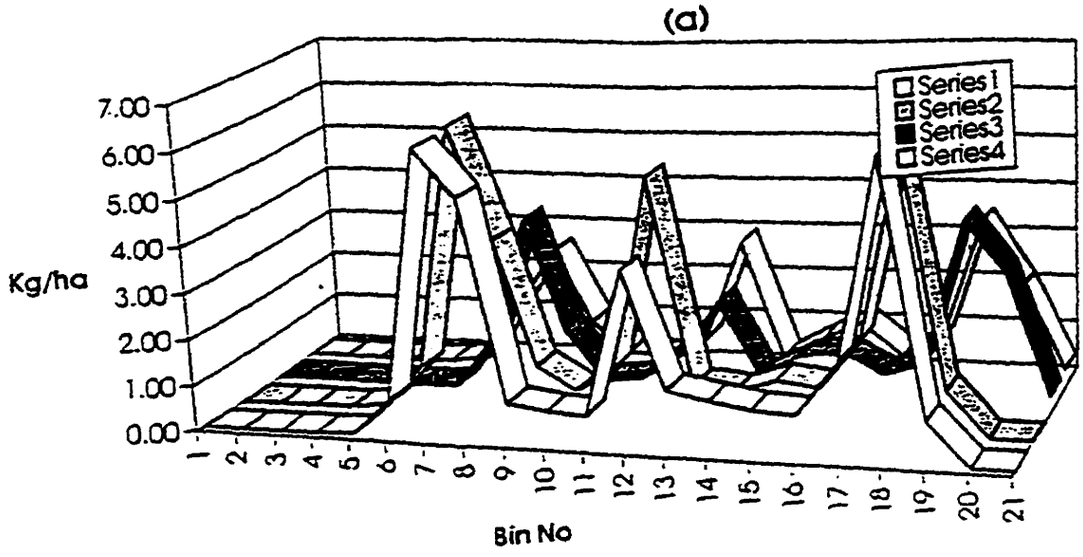

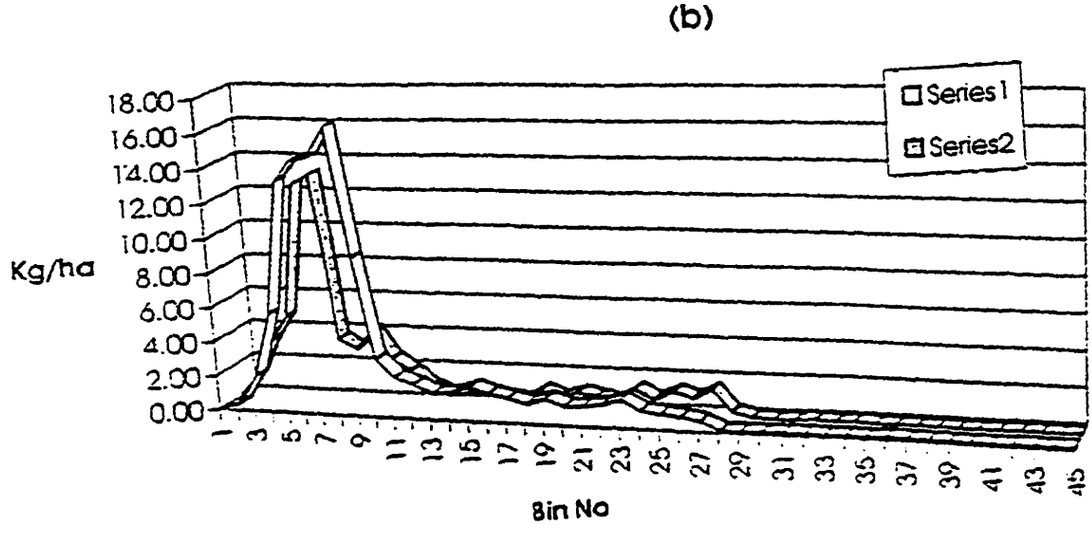

Figure 4.8: Test 7: (*a*) Pattern Across the Swath: (*b*) Pattern Along the Swath.

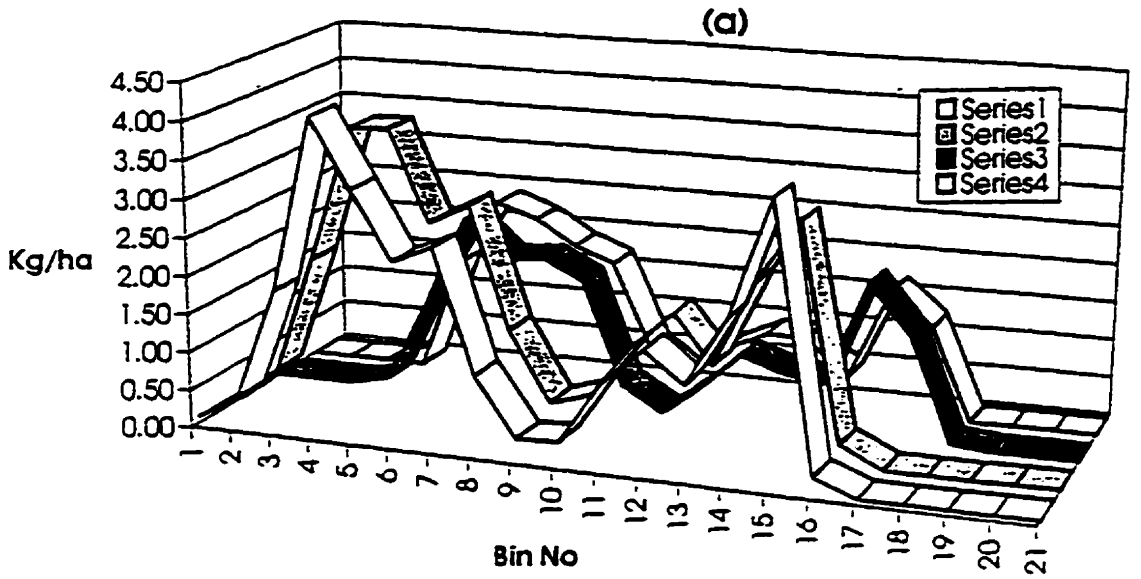

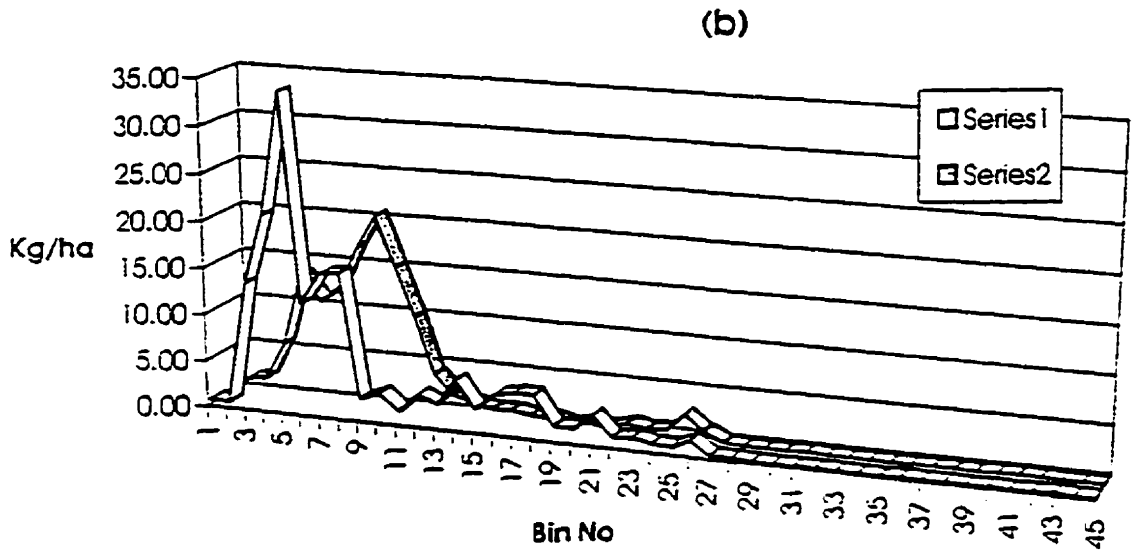

Figure 4.9: Test 3: (*a*) Pattern Across the Swath: (*b*) Pattern Along the Swath.

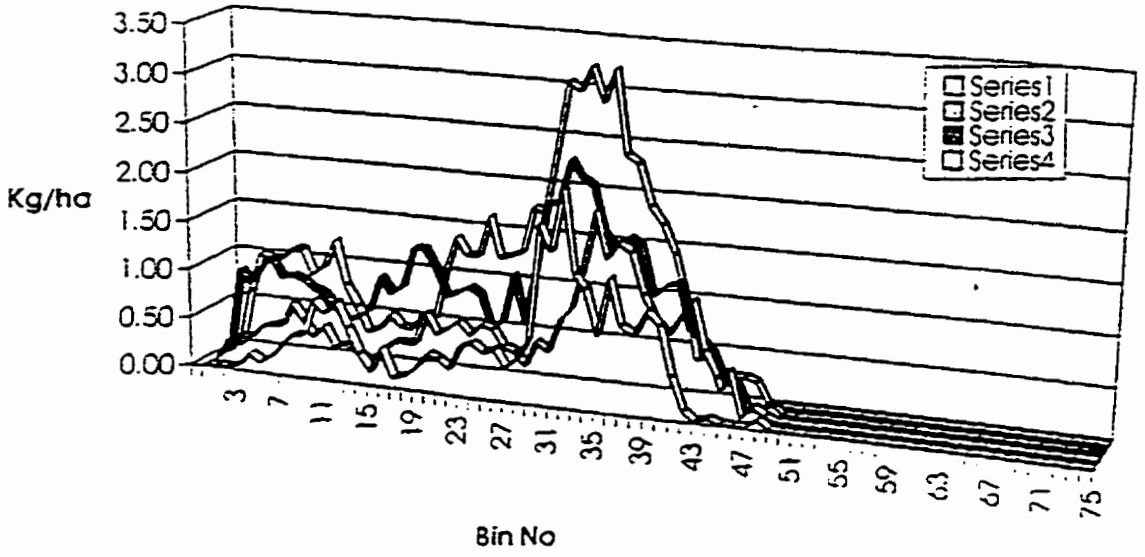

Figure 4.10: Test 9: Pattern Across the Swath.

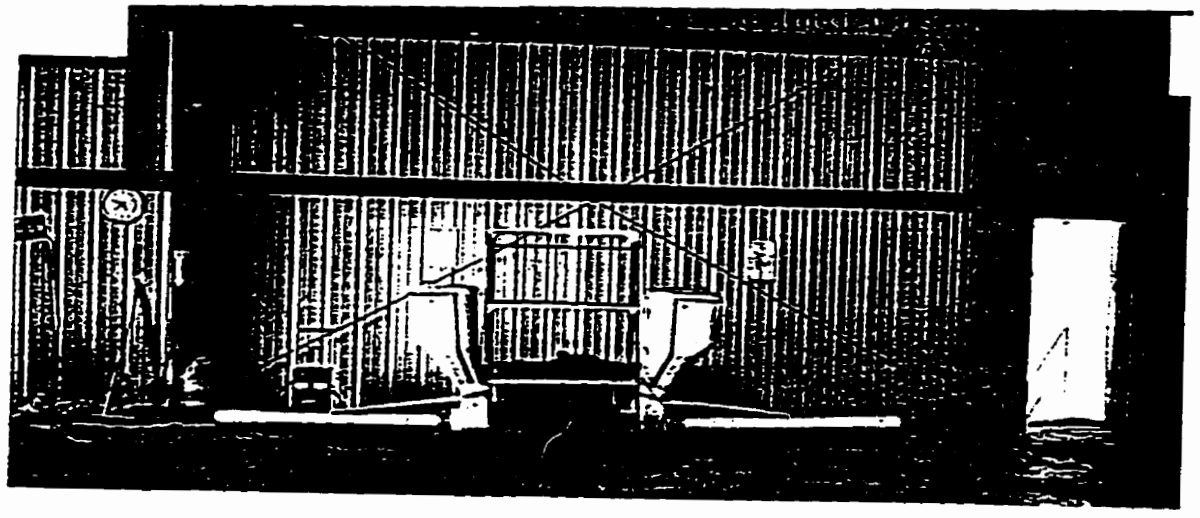

Figure 4.11: Stationary Test Station

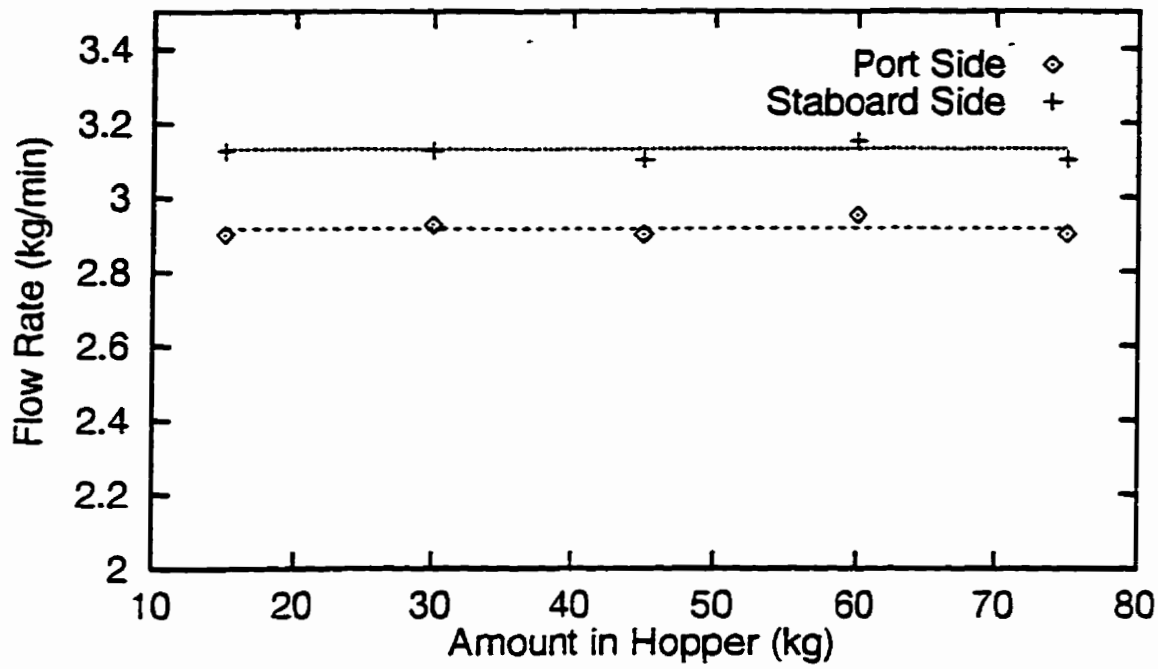

Figure 4.12: Hopper Level vs. Flow Rate.

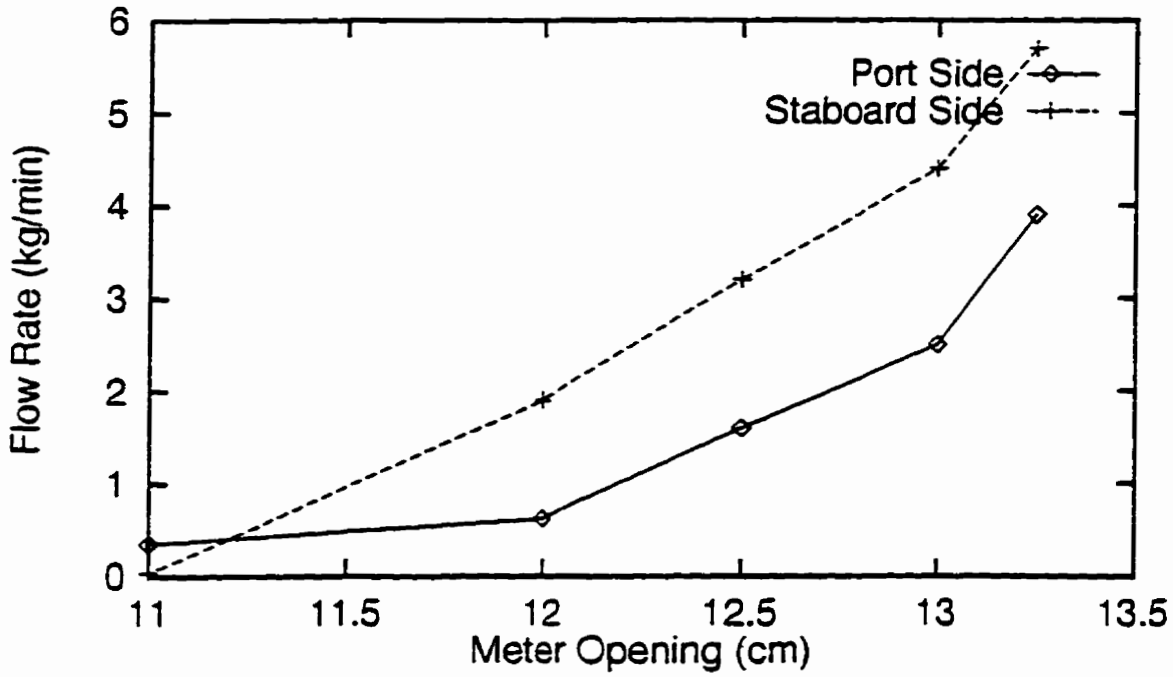

Figure 4.13: Meter Opening vs. Flow Rate.

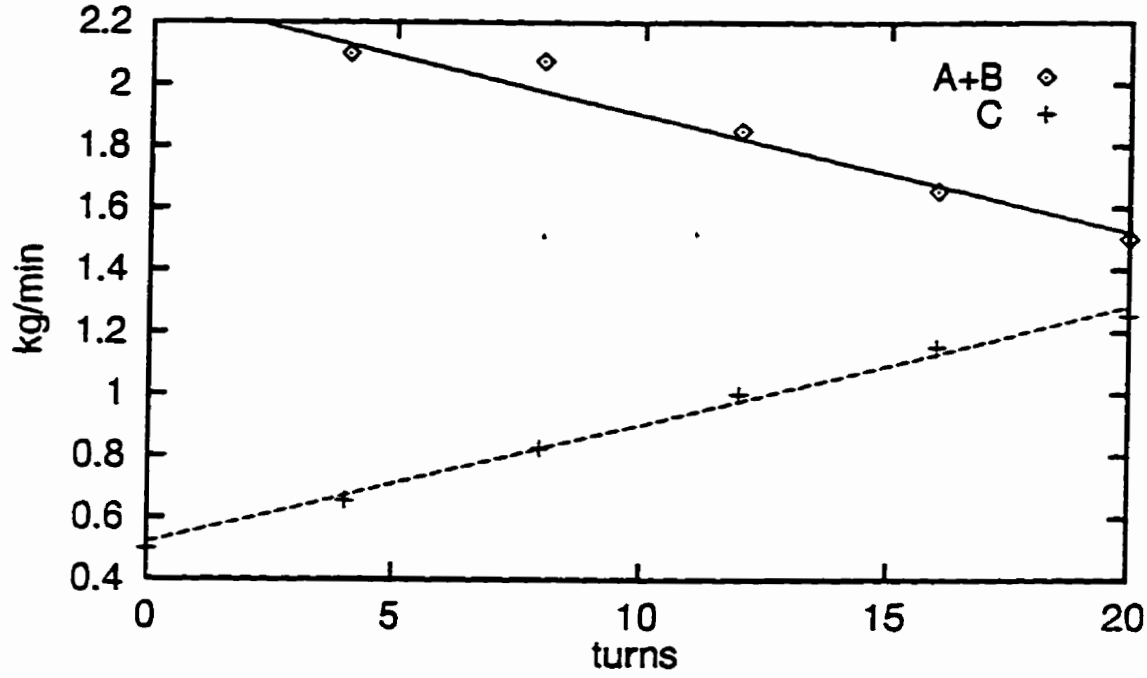

Figure 4.14: Deflector 'C' Position vs. Flow Rate.

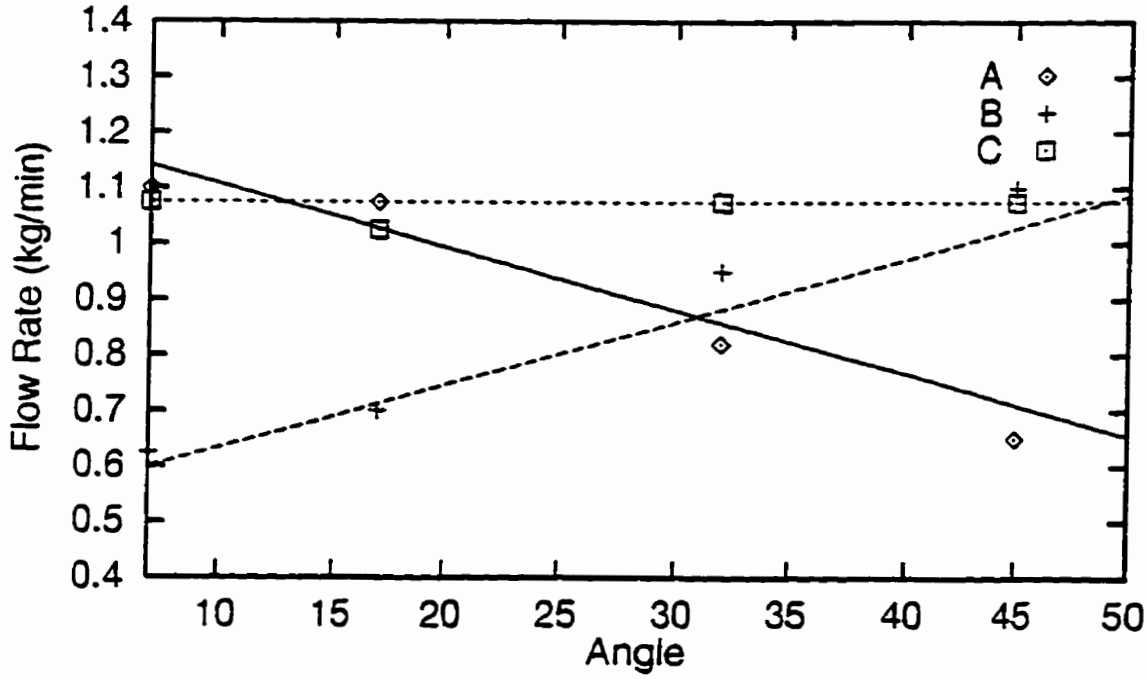

Figure 4.15: Deflector 'B' Position vs. Flow Rate

Chapter 5

Simulation Study

5.1 The Particle Trajectory Model (TRAJECT)

The single particle equations of motion described in Chapter 3.1 is now utilized to develop a computer program called TRAJRCT, to simulate the trajectory of a particle ejected from a height. The effect of particle properties (size and density), ejection velocity, and altitude on the trajectory and the range of a particle are studied using this program. The range of a particle is defined as the perpendicular distance from the flight line covered by a particle before it reaches the ground.

The equations of motion (3.9) to (3.11) are to be solved numerically. The classic fourth order Runge Kutte is used to perform the numerical integration. The initial velocity of a particle is calculated using equations (3.1) to (3.4). The coefficient of drag is calculated at each step from the current value of the Reynolds number. The calculation stops when the partical reaches ground. The total distance moved along the horizontal axis gives the range of the particle.

5.1.1 Effect of Particle Physical Properties

The effect of two of the most important physical properties. namely, size and density, are studied. The size of a spherical particle has two opposing effects on the range of a particle. The drag force. F, as given by equation (3.8) is directly proportional

to the diameter of a particle. Thus a larger particle experiences more drag force, which reduces the range. On the other hand the left hand sides of equations (3.12) to (3.14) represent the inertial force acting on the particle. The inertial force is directly proportional to the mass of a particle (Newton's second law of motion). Since the mass of a spherical particle is proportional to the cube of the diameter, an increase in size of a particle increases the range of the particle. Figure 5.1 shows the effect of particle diameter on the trajectory. Consistent with the theory, it is observed that the larger sized particles travel father than the smaller ones.

The density of a particle affects the mass of the particle. A denser particle has higher mass for the same size of a lighter particle. Thus an increase in density of a particle increases the range, as depicted in Figure 5.2.

5.1.2 Effect of Ejection Velocity and Altitude

Particles with a higher initial velocity travel farther due to their inertia. Figure 5.3 shows a number of trajectories of a particle with different initial velocity.

The altitude of the particle ejection may affect the range if the particle reaches the ground before its motion is purely vertical. From Figures 5.1, 5.2 and, 5.3 it is observed that the particle motions are vertical for all practicle purpose well before the particle hits the ground. Therefore, unless the altitude of ejection is very low (application from spreader attached to ground vehicles) the range of the particle is not affected much by a change in altitude of the flight.

5.1.3 Summary

Figure 5.4 depicts the effect of the exit velocity, particle size and density on the range of the particles. It may be summarized that in order to get larger spread, (*i*) particle size should be increased, (*ii*) particle density should be increased, (*iii*) ejection velocity should be increased and, (*iv*) altitude should be high enough so that the particle have no or negligible motion in the horizontal direction. However, it may be noted that larger particle size and density means fewer particles per unit area on the field, and this may affect the effectiveness of the chemical. Higher ejection velocity requires higher kinetic energy input, which may or may not be justified depending upon particle density and size. Thus a careful selection of these variables is needed to get the best possible spread. Program TRAJECT is helpful to the aerial solid material applicators in such selection processes.

5.2 The Deposition Model (DEPOSIT)

Though helpful in studying the effect of various variables on the travel of a particle the particle trajectory program in itself does not provide information about the deposition pattern of the particle. The deposition pattern depends not only upon the individual particle properties like size and density, but also on the make of the spreader, flow rate, altitude, wind velocity, and aircraft speed (Bouse, 1985).

In the present arrangement, the variables pilot can change while flying is the helicopter speed, direction, and altitude. Change in aircraft speed would changes the average deposition rate (D_R). D_R is related to the aircraft speed (V_G), swath width (S) and the total chemical flow rate (Q), by the following relation:

$$D_R = \frac{Q}{V_G S} \tag{5.1}$$

The altitude of the flight will not affect the deposition rate directly. However, if the altitude is very low then particles may reach the ground with horizontal component of the velocity still high enough to reduce the effective swath width.

It is observed, from the particle trajectory simulation, that the initial direction and velocity of a particle has a very important role in deciding the ground impact location of the particle. Determining each particles speed and direction as it comes out of the spreader is out of scope of the present study. The experimental determination of the particle velocity and direction requires extensive instrumentation and excessive signal processing (Hofstee, 1994). Hofstee reported a scheme of using ultrasonic transducers utilizing Doppler shift, needed about 15 hours of processing time to process all the data associated with a measurement lasting about 3 minutes.

Consistent with the previous work (Gardisser, 1992) the exit velocity of particles is taken as the 60% of the measured air velocity at the exit. With the help of a inclined tube manometer, the average velocity of air at the exit was measured to be 20 $\frac{m}{s}$ for the spreader under study. The particle coming out of an exit was assumed to follow the direction of the exit.

The DEPOSIT program first classifies the particle into finite size categories assuming a normal distribution. Taking initial particle velocity of 60% of the measured spreader air-velocity and the direction same as the direction of the outlet. the trajectory of each size class is determined for all the outlets using the single particle equations of

motions. Such model, as expected, will indicate that all the particles from an exit, belonging to a size group, impact at exactly one location on the ground. In reality this is not expected to be true. That is because there is always slight differences in particle size, shape, mass, initial release direction, air turbulence etc. that introduce randomness in the impact location.

In the model developed by Gardisser (1992), the impact location was assumed to approximate a Gaussian distribution curve. Similar approach has been adopted here. The program determines the expected impact location of each size category of the particle using the TRAJECT program and then normalizes the impact location to account for the uncertainty. This is done for each outlet and finally the particles impacting over a range ($1\ m \times 1\ m$) of swath is summed together. This amount when divided by the simulated collection area gives the expected deposition rate at a particular location. A set of data input for a typical run of DEPOSIT program is given in Table (5.1).

Figure 5.5 shows the predicted pattern for standard operating condition. We define standard operating condition as 50 ft helicopter altitude, 80 $\frac{km}{hr}$ speed, 3 $\frac{kg}{min}$ flow rate and no atmospheric wind.

Figure 5.6 depicts the pattern when helicopter speed is increased to 120 $\frac{km}{hr}$. Higher helicopter speed affects the pattern in two ways; firstly, it results in a lower deposition per unit area as the helicopter covers more area in a given time: secondly, the swath becomes narrower as the particles tend to move along the direction of the flight. The simulated pattern shows these trends.

Figure 5.7 shows the predicted pattern if the altitude of the flight is very low (10 ft). The lower altitude application may lower the swath width as particles are unable to achieve their full range. The deposition uniformity is also affected as particles have less time to diverge from each other after they emerge together from the exit. The very high deposition at the middle of the pattern and a slight reduction of the swath width can be noted in the Figure. Figure 5.8 gives the predicted deposition pattern if a cross wind of 2 $\frac{m}{s}$ is present while applying. Pattern has shifted from the flight line due to the presence of the wind.

The advantage of a simulation model is the ability to experiment with different combinations of the spreader geometry and material properties. Figure 5.9 shows the effect of varying the angle β of the exit "C" (refer Figure 1.3) on the deposition pattern. For clarity two dimensional deposition plots are used here-forth. As can be seen in the Figure, 65 degrees gives the best possible result. Figure 5.10 shows the effect of the angle β of the exit "B". An angle of 30 degrees or more contributes positively towards the better spread of the particles.

The effect of the particle size distribution is shown in Figure 5.11. The Gaussian distribution with larger standard deviation helps in achieving better spread. Figure 5.12 shows the deposition pattern when 4 outlets placed at equal interval, with equal flow rate of material and with same exit angle is simulated. As seen in the Figure, this deposition pattern does not have better uniformity when compared with the pattern with three outlets and optimum settings. Thus, if the exit angles and the percentage of material through each exit is elected carefully, it is not necessary to increase the number of ports.

One of the observations of the field test was, dispersal tubings which were used to direct the material towards the center of the pattern play an important role in achieving better deposition uniformity (Chapter 4.1.4). Figure 5.13 shows the deposition patterns with and without the tubes. As seen in the Figure, the tubes help the center of the pattern receive the material.

5.3 Comparison of Simulated patterns with the Test Patterns

Tests results executed under ideal conditions (no disturbance owing to wind, no change in meter setting due to vibrations, no judgemental error by pilot in maintaining the specified altitude, line of flight and speed) are needed for validation of simulation model. Since such test data are unavailable, tests data obtained by conducting field tests as described in Section 4.1 are used for the comparison.

For each set of input (flight speed, altitude, application rate and cross wind) there are four test patterns (two rows of collection bins and two passes over them). The average of the two rows is used for the comparison. The simulation program produces a unique pattern for one set of input. Since there is considerable variation from one test flight to another, the test pattern of both flights are compared.

The cross wind causes the pattern to shift in its direction. To account for the effect of cross wind, the cross wind velocity in the model input is selected such that the test pattern and the model pattern center are matched approximately.

The comparison for tests 1 to 8 are presented in Figures 5.14 to 5.21. Only the

distribution pattern of a cross section of the flight is shown. Figure 5.14 shows the comparison for the standard condition (50 $ft.$ altitude, 80 $\frac{km}{hr}$ helicopter speed, and 3 $\frac{kg}{min}$ application rate). A portion of the swath has been lost probably due to the cross wind present. The test pattern for the first flight shows smaller average deposition rate as compared to the predicted pattern. The reason may be since this test was conducted on early morning, the granules absorbed moisture from the atmosphere and many got dissolved on impacting the hard plastic surface of the collectors. The simulated pattern has narrower swath width than the test patterns. The down-wash from the helicopter rotor may have contributed to the spread of the particles. This effect is not included in the model. Both the test patterns and the predicted pattern have a high peak on the side from which wind is blowing (left to right).

When the altitude is reduced to 25 ft, keeping other variables constant, the swath has reduced for test pattern as expected (Figure 5.15). The simulated pattern still shows about the same swath width. The reduction in test pattern swath width is due to the particles having less time in air and thus minimizing the effects of the atmospheric and rotor wind.

The test with 100 ft shows an increase of the swath as shown in Figure 5.16. The cross wind may have changed significantly from the time of first flight to that of second flight. The test patterns are well spread over the swath. High altitude application thus facilitates the spread of the particle. High altitude application is affected more by any cross wind present.

Figure 5.17 depicts the comparison when the helicopter speed is reduced to 70 km/hr, keeping other variables at standard condition. The reduction in speed should

result in higher deposition rate. The test pattern does not show this but the simulated pattern shows an increase in deposition rate. When the speed is increased to 90 $\frac{km}{hr}$ (Figure 5.18), the decrease in deposition rate is predicted by the simulated pattern.

The pattern with increased rate of chemical (6 $\frac{kg}{min}$) and the predicted pattern is as shown in Figure 5.19. The increase in deposition rate is predicted by the simulation pattern. Figure 5.20 shows the comparison, when the innermost outlet at each side was removed. These tubes are used to direct the chemical towards the center of the flight line. Figure 5.21 shows the comparison for the similar setup but the rate of chemical reduced to 3 $\frac{kg}{min}$. The deposition rate has not decreased for the test patterns. This may be due to the incorrect calibration of the flow mete or change of settings after the calibration. The test patterns exhibit a steeper peaks and valleys.

Thus the qualitative graphical comparisons of the simulation model predictions with observations made during the field tests, indicate that the model has some skills in predicting general trends in some of the features (magnitude of peaks, effect of cross wind and, the swath width) in the observations. Uncertainties in source and meteorological inputs probably help to explain the discrepancies.

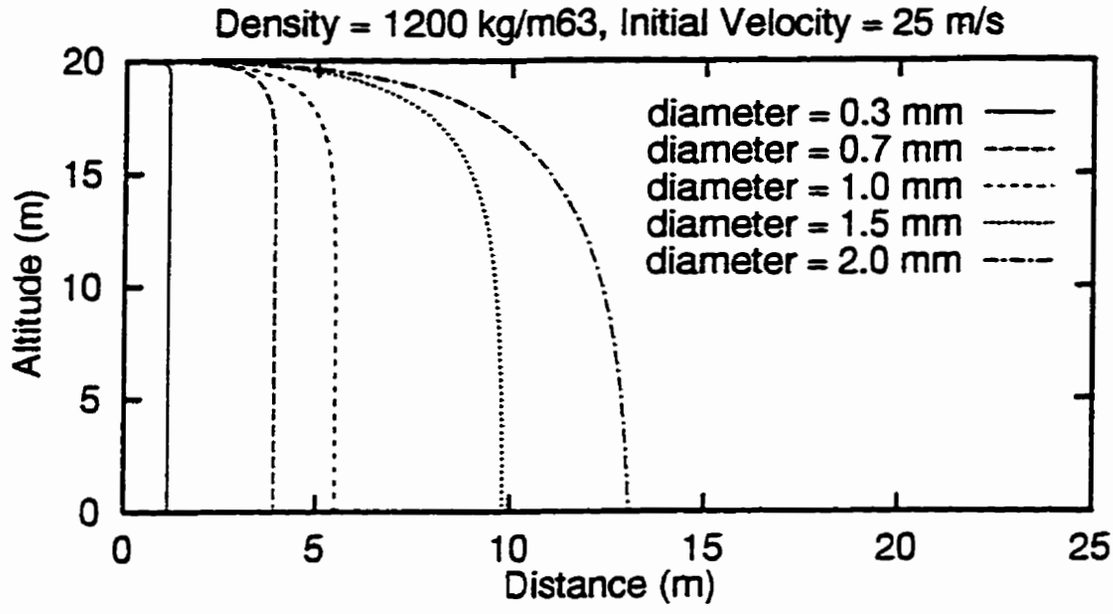

Figure 5.1: Effect of Size of a Particle on the Trajectory.

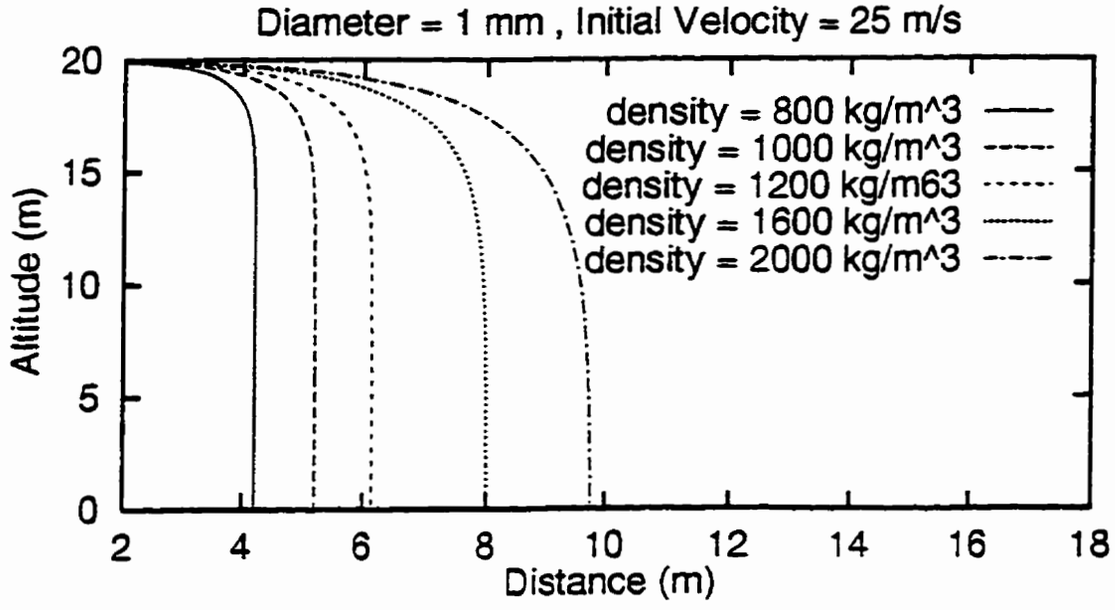

Figure 5.2: Effect of Density of a Particle on the Trajectory.

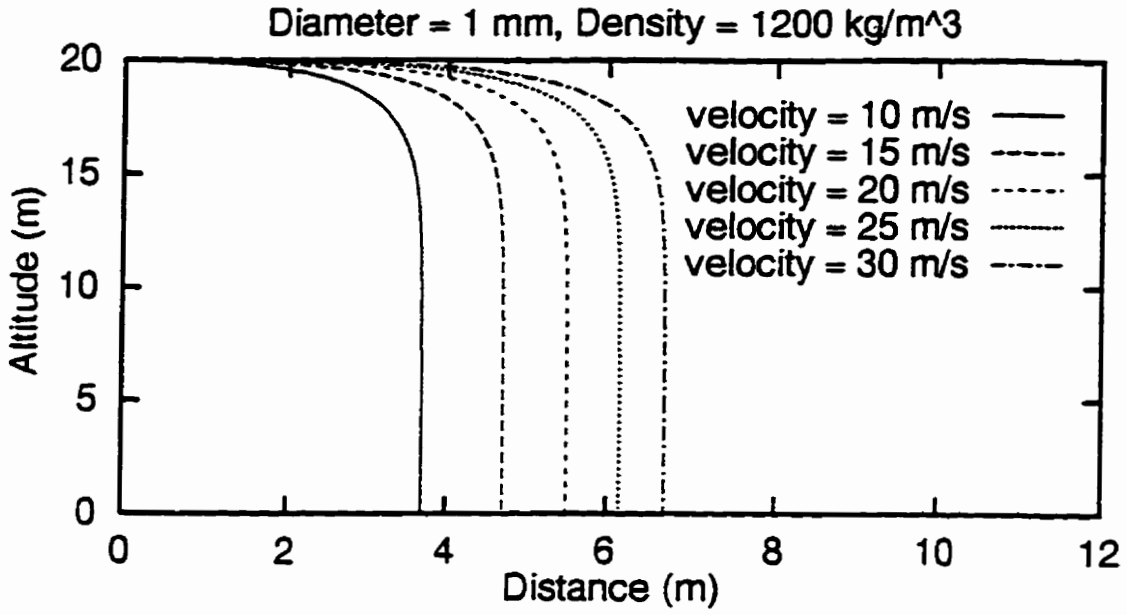

Figure 5.3: Effect of Initial Velocity of a Particle on the Trajectory.

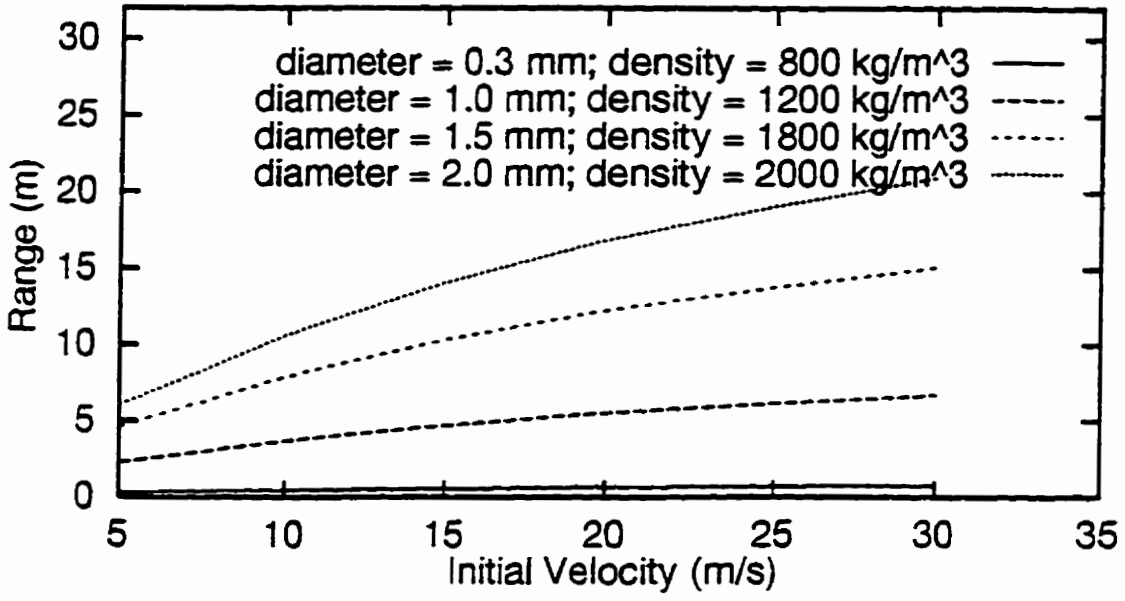

Figure 5.4: Effect of Size, Density and. Initial Velocity on the Range.

Table 5.1: Input Data for a Run of DEPOSIT Program.

Variable	Meaning	Typical value
ALT	Altitude of the flight	50 ft
V_G	Helicopter speed	80 $\frac{km}{hr}$
ANGLE	Angle of ejection with the horizontal plane	0.0
ANGLE1	Angle of ejection with the vertical plane	45
Rate	Flow rate (Total)	3 $\frac{kg}{min}$
PD	Particle density	1200 $\frac{kg}{m^3}$
AD	Air density	1.225 $\frac{kg}{m^3}$ at 20 C
VE	Average exit velocity of the particles	12 $\frac{m}{s}$
TEMP	Air temperature	20 C
MEANP	Average particle size	1 mm
WIND	Cross wind velocity	1 $\frac{m}{s}$
Winddir	Wind direction	90 degree
BINS	Number of bins	41
SIMTIME	Simulation time	1 s
SIZE	Mean size of the particle	1 mm
SDP	Standard deviation of the size distribution	0.2
SDL	Standard deviation of the location distribution	2

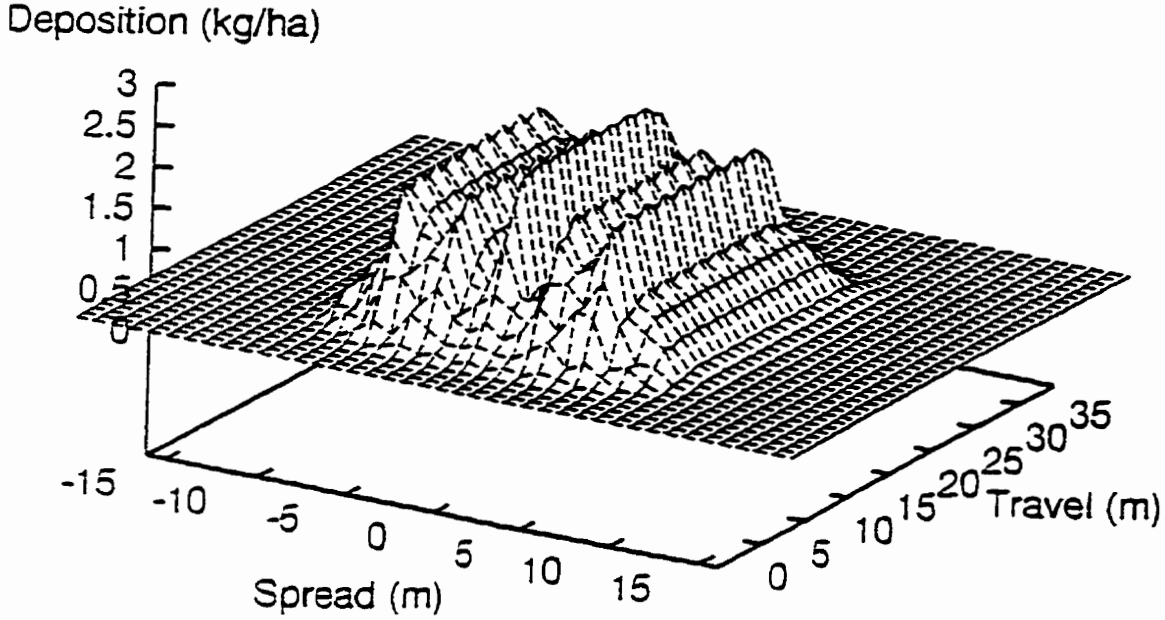

Figure 5.5: Simulated Pattern for Standard Operating Condition.

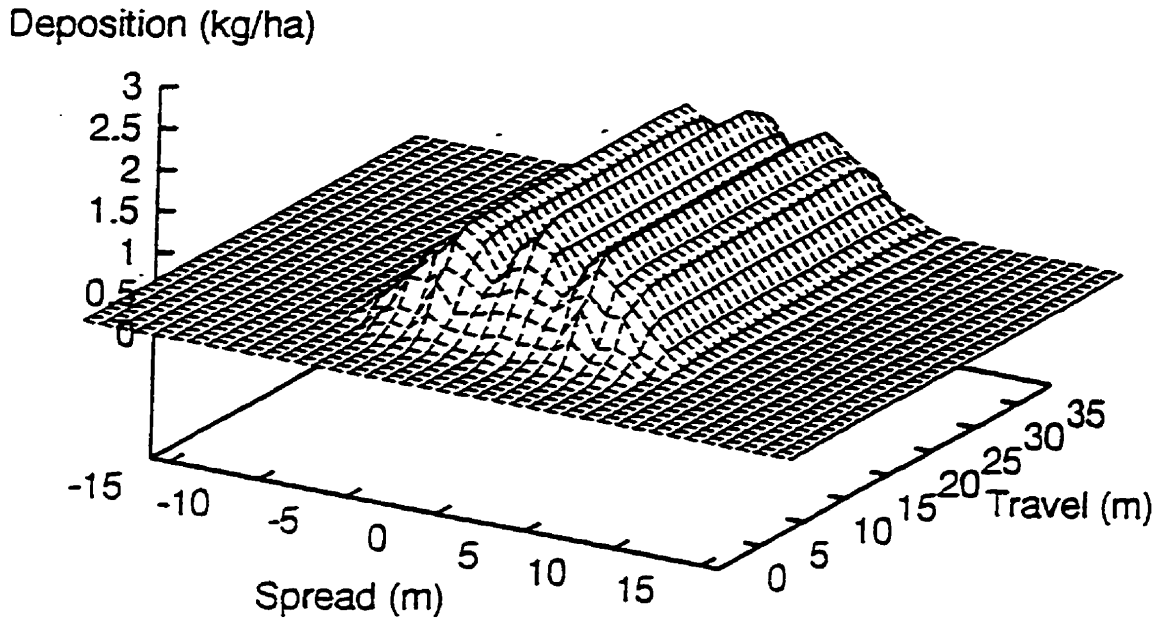

Figure 5.6: Simulated Pattern for Higher Helicopter Speed

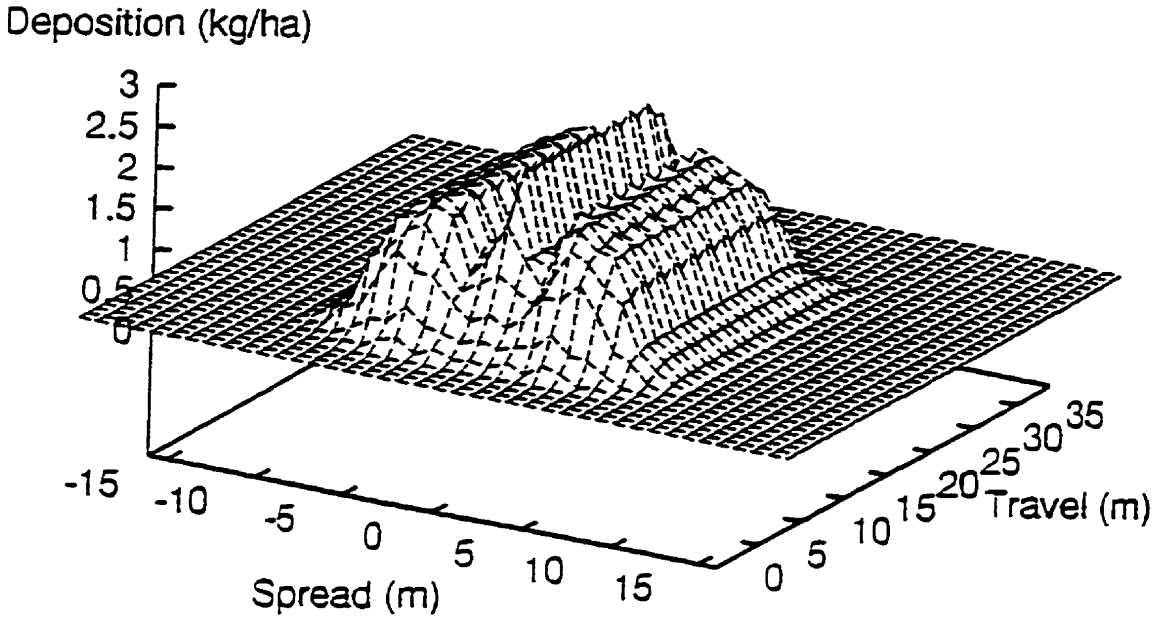

Figure 5.7: Simulated Pattern for Low Altitude

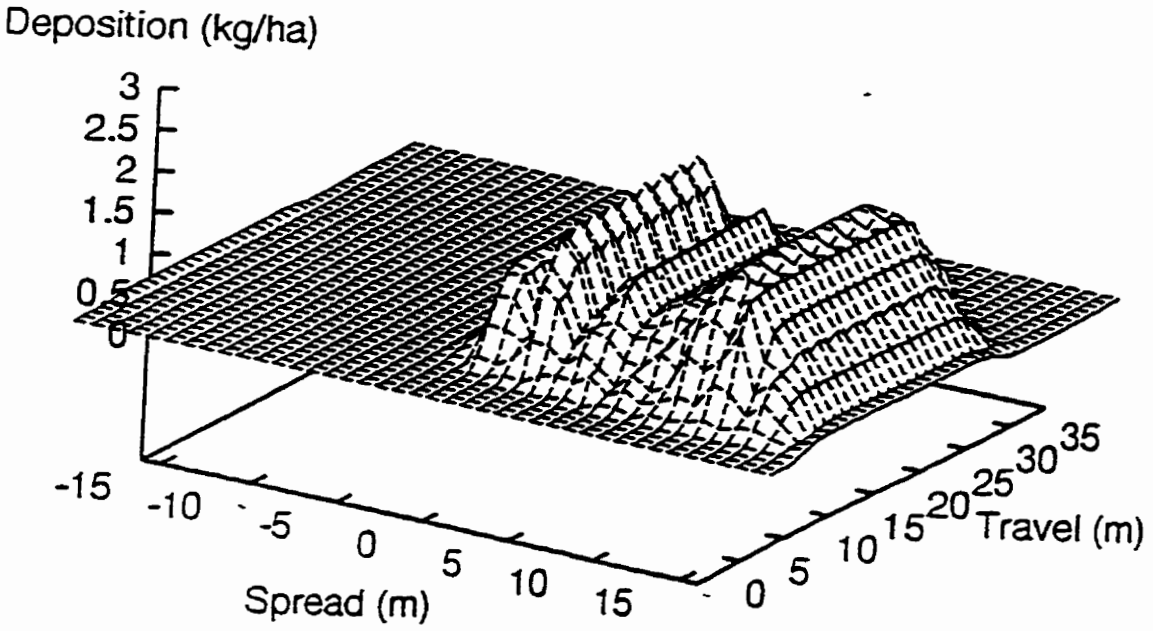

Figure 5.8: Simulated Pattern in the Presence of Cross Wind.

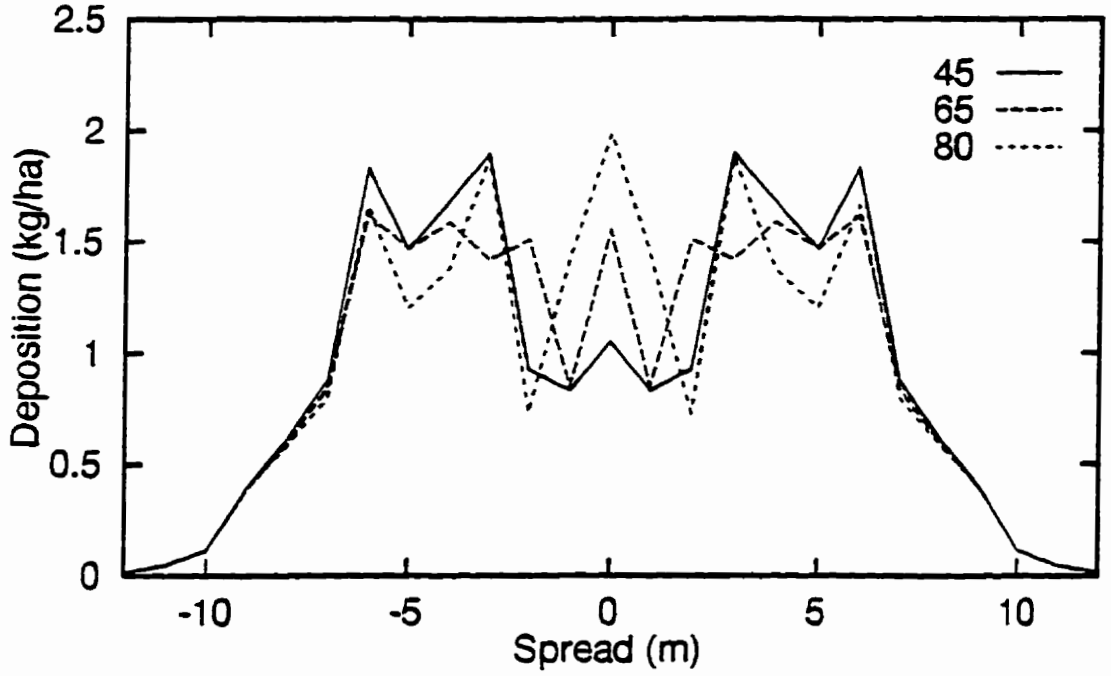

Figure 5.9: Effect of Exit "C" Angle on the Deposition Pattern (Standard Condition, Mean Size = 1 mm, SD = 2, Angle of "B" = 45).

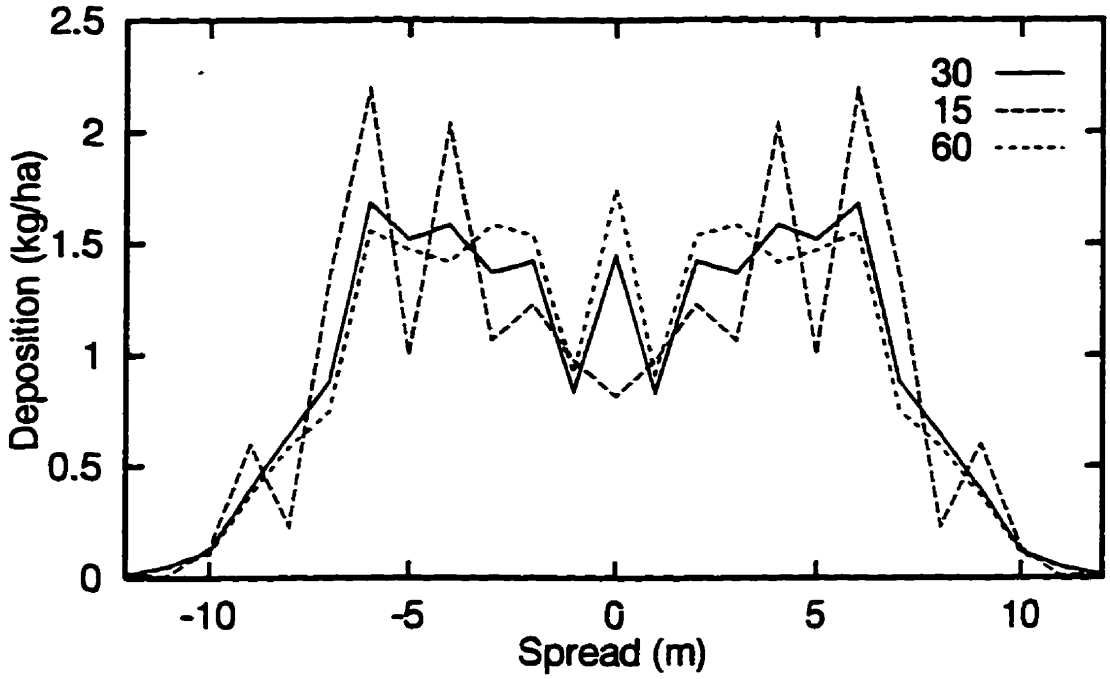

Figure 5.10: Effect of Exit "B" Angle on the Deposition Pattern (Standard Condition, Mean Size = 1 mm, SD = 2, Angle of "C" = 65).

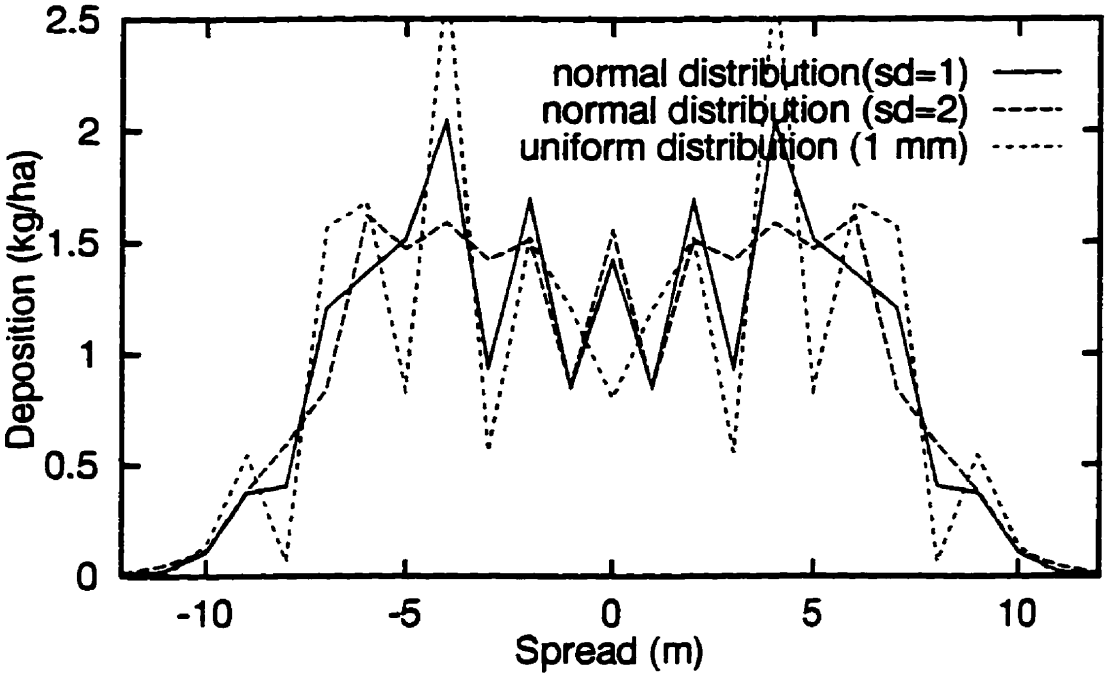

Figure 5.11: Effect of Size Distribution on the Deposition Pattern (Standard Condition, Angle of "B' = 30, Angle of "C" = 65).

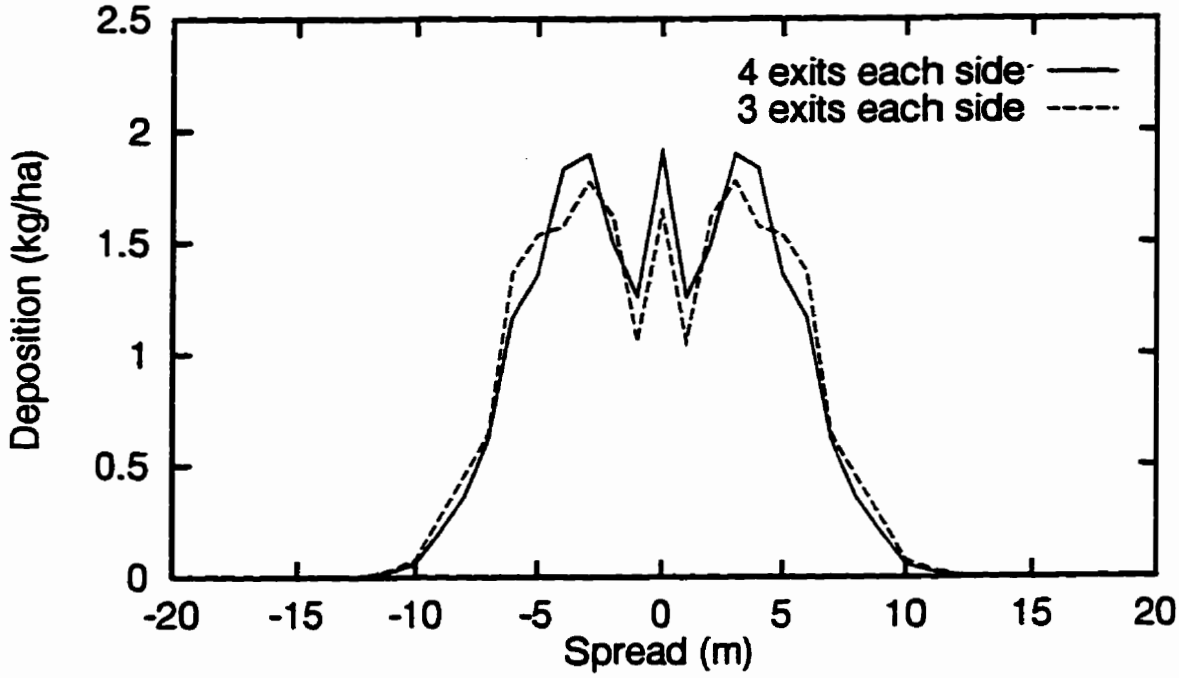

Figure 5.12: Effect of Number of Exits on the Deposition Pattern (Standard Condition).

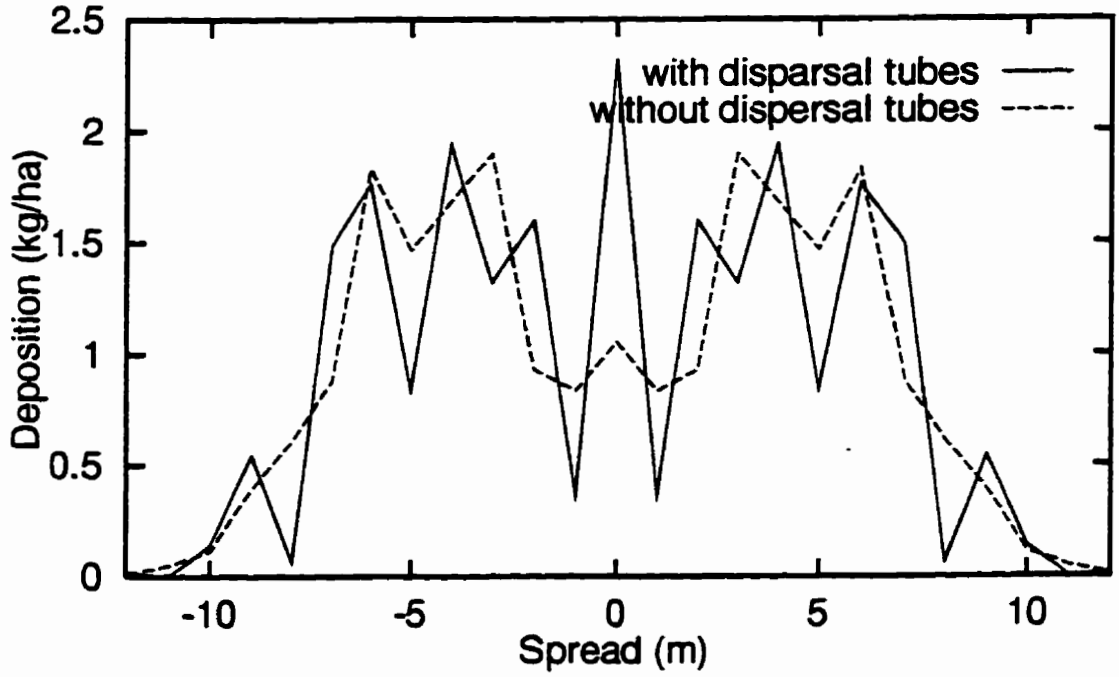

Figure 5.13: Effect of Spreader Tubes on the Deposition Pattern (Standard Condition)

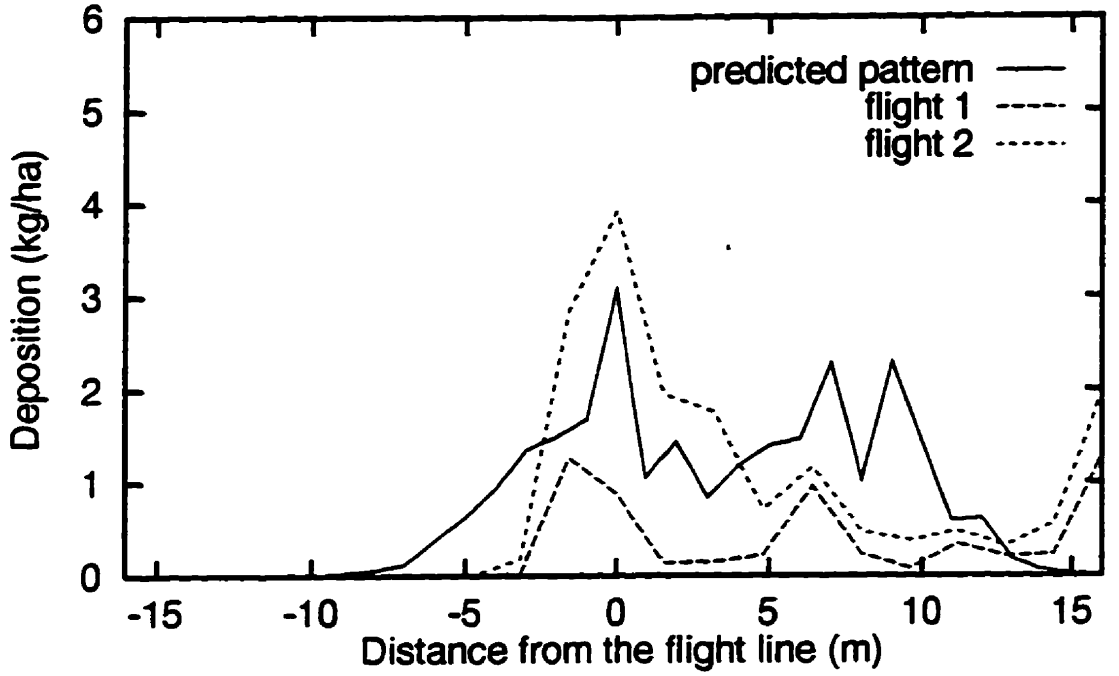

Figure 5.14: Field Pattern vs. Predicted Pattern; Test 1 (Standard, Cross Wind = 0.75 $\frac{m}{s}$).

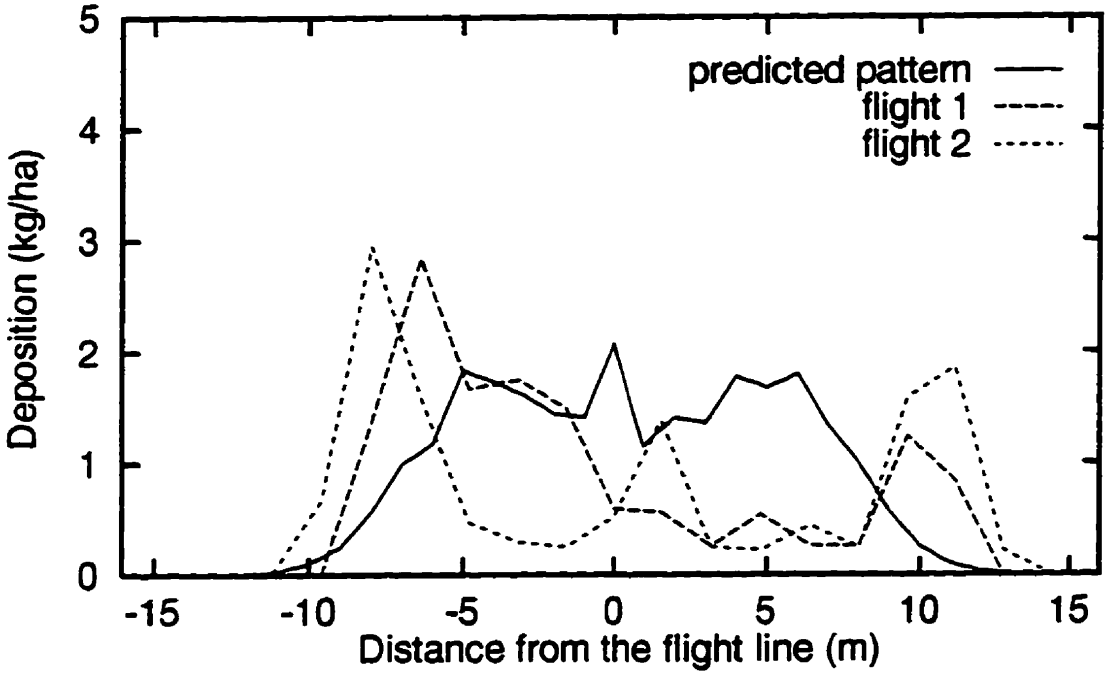

Figure 5.15: Field Pattern vs. Predicted Pattern; Test 2 (Altitude = 25 ft, Cross Wind = 0.25 $\frac{m}{s}$).

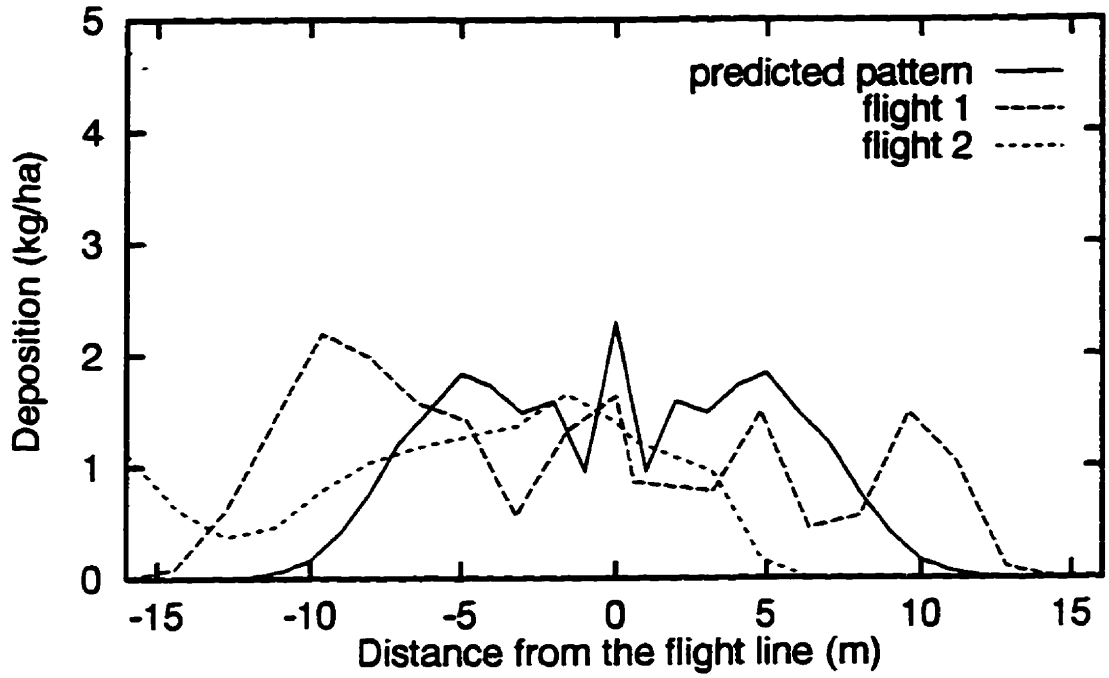

Figure 5.16: Field Pattern Vs. Predicted Pattern; Test 3 (Altitude = 100 ft, Cross Wind = 0.0 $\frac{m}{s}$).

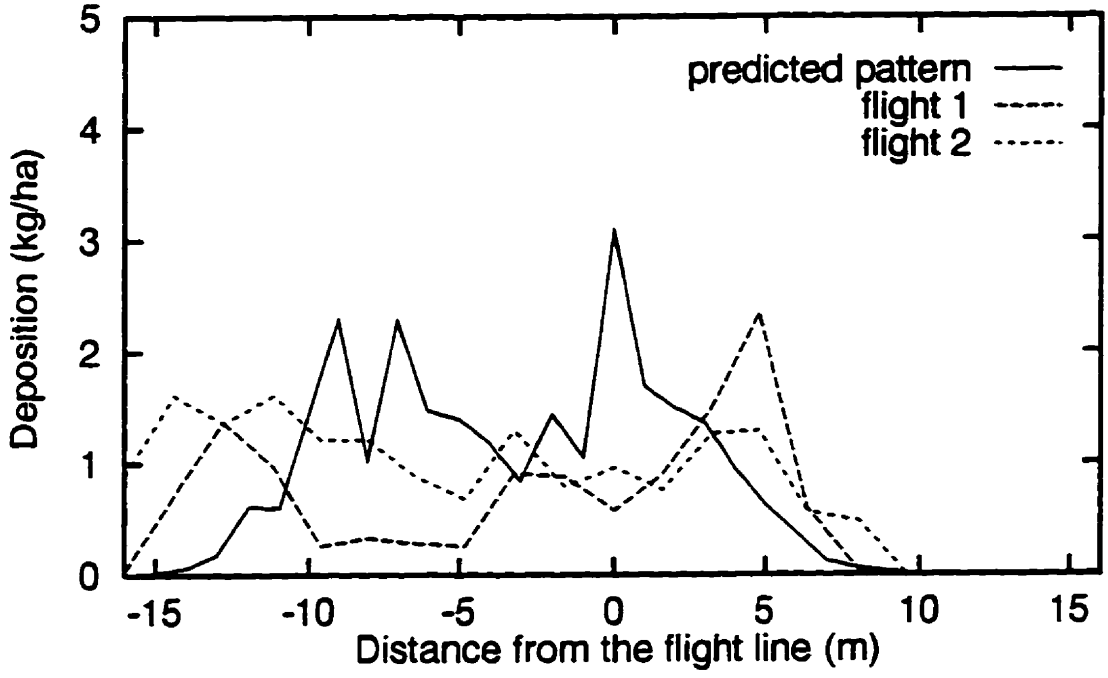

Figure 5.17: Field Pattern vs. Predicted Pattern; Test 4 (Speed = 70 $\frac{km}{hr}$, Cross Wind = -0.75 $\frac{m}{s}$).

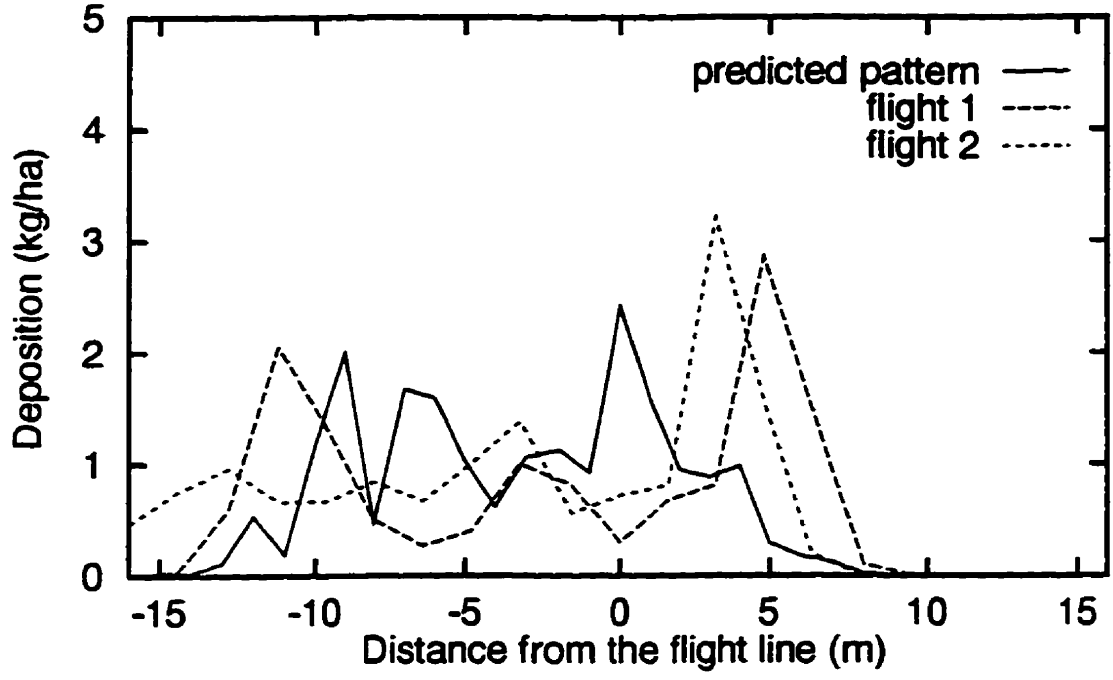

Figure 5.18: Field Pattern vs. Predicted Pattern; Test 5 (Speed = 90 $\frac{km}{hr}$, Cross Wind = -0.75 $\frac{m}{s}$).

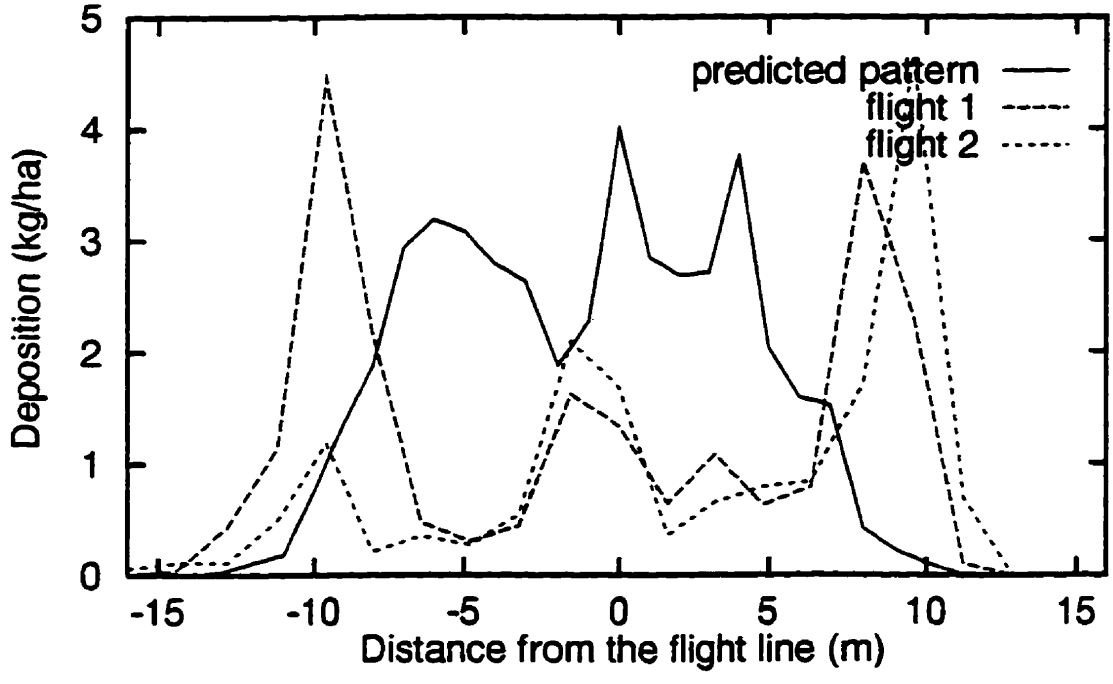

Figure 5.19: Field Pattern vs. Predicted Pattern; Test 6 (Rate = 6 $\frac{kg}{min}$, Cross Wind = -0.5 $\frac{m}{s}$).

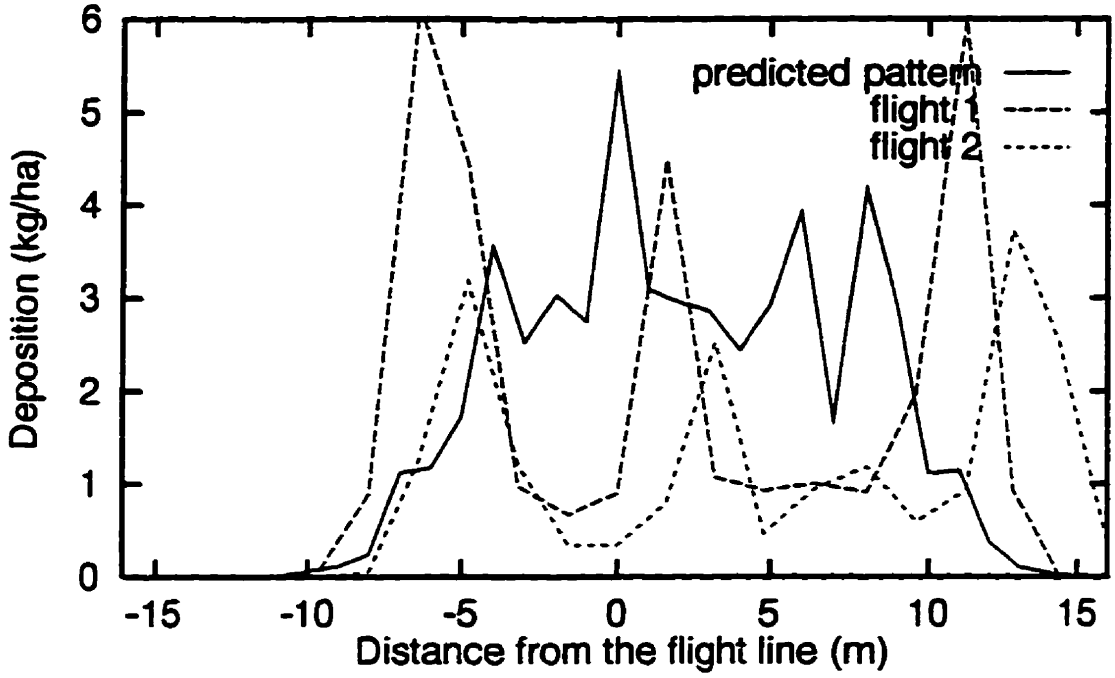

Figure 5.20: Field Pattern vs. Predicted Pattern; Test 7 (Dispersal Tubes Removed, Rate = 6 $\frac{kg}{min}$, Cross Wind = 0.5 $\frac{m}{s}$).

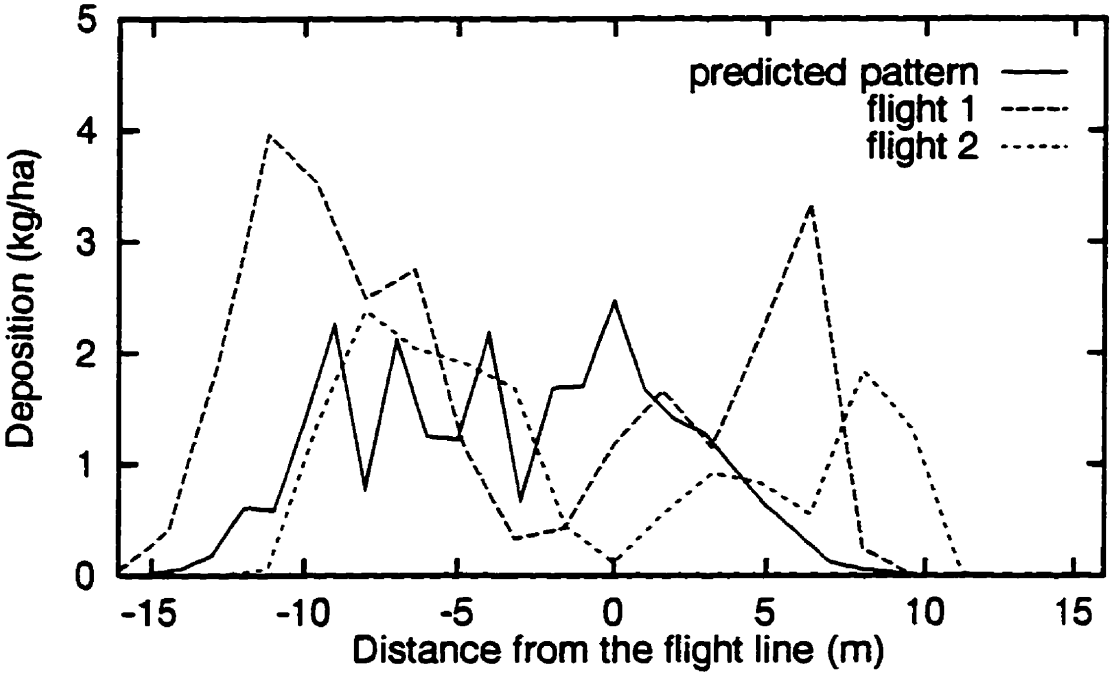

Figure 5.21: Field Pattern vs. Predicted Pattern; Test 8 (Dispersal Tubes Removed. Rate = 3 $\frac{kg}{min}$, Cross Wind = 0.75 $\frac{m}{s}$).

Chapter 6

Concluding Remarks

6.1 Conclusions

Ground deposition patterns of granular particles applied from a class of helicopter borne spreader were studied in this thesis. First of all a mathematical model was developed to calculate trajectories of spherical solid particles ejected from an altitude. This model takes into account the gravitational, inertial, and drag forces. Empirical relation to predict the coefficient of drag for a wide range of Reynolds number was identified and was used to calculate the drag force. This method facilitated quick and convenient determination of trajectories.

A computer simulation program (TRAJECT) was developed and used to study the effects of changing the particle size, density, initial velocity and altitude of ejection on the trajectories and the spread of the particles. The simulation results showed that heavier and larger particles increase the spread. The initial velocity with which the particles are ejected have direct effect on their spreads. It was also observed that for lighter and smaller particles an increase in the ejection velocity may not result in significant increase in the spread. The particles in the size range (0.3-1.5 mm), attained full horizontal spread within the first 10 m travel in vertical direction. For particles in this size range any increase in altitude beyond 10 m will have very little effect on their range.

A second computer program (DEPOSIT) was then developed to simulate the ground deposition pattern. DEPOSIT gives a 3-dimensional view of the expected ground deposition pattern if the helicopter speed, altitude, material flow rate and the material properties like size and density are given. Simulation studies using this program demonstrated that a higher helicopter speed would decrease the deposition rate if the flow rate was kept constant. The cross wind was found to affect the pattern shape and location significantly. In a past study it was assumed that the sole effect of cross wind would be that of shifting of the pattern (Gardisser, 1992). The simulation study with DEPOSIT suggested that the shape of the patterns are altered by the cross wind. The simulation studies also showed that it was possible to improve the deposition uniformity by adjusting the exit geometry settings. DEPOSIT is expected to be a valuable tool in future development of control system, so that the rate of application could be varied as the field need and/or the flying condition changes.

Field tests were also conducted to obtain the actual field deposition pattern. Both along the flight and across the flight pattern are obtained. The pattern along the flight detected a problem previously unreported. The pattern showed a very high application rate at the beginning of the application. This was not observed during the test of the stationary spreader. The tests on the stationary spreader showed that amount of chemical in the hopper had no effect on the flow rate of the chemical for the range of the test (15-75 kg). The sliding plate mechanism was found to be inadequate to control the flow rate of in the neighborhood of 1 kg/min consistently. However, it was found that, the material metered from the hopper could be deflected to follow the three exits on each side by using the set of deflector plates "B" and "C".

A comparison between the simulation results and the field tests indicated that the computer model has the potential to predict some of the characteristics of the deposition pattern. Model could predict the trends in the effect of changes in helicopter speed, altitude, particle properties, flow rate and cross wind. The number of peaks and valleys and the swath width was also indicated by the model to some extent.

6.2 Recommendations for Future Work

More work is required to validate the simulation model. An indoor test station to collect data under controlled condition will help in better understanding of the deposition process. Further work on accurate method (analytical or experimental) method to calculate initial particle speed and direction will make the impact location prediction more accurate.

The flow meter is a prime target for improvement. Future work should be focussed on developing a variable rate flow meter. A control system could then be added so that the meter could adjust the flow rate under varying conditions.

References

1. Akesson, N.B., Yates, E.W. 1974. "Use of Aircraft in Agriculture," FAO Agricultural Development Paper No-94, Food and Agriculture Organization of the United Nations.

2. ASAE, 1988. "Calibration and Distribution Pattern Testing of Agricultural Application Equipment," ASAE Standard, ASAES 386.2, St. Joseph, Michigan.

3. Barnes, B.M., J.T. Walker, and D.R. Gardisser. 1991. "Effects of Fertilizer Particle Properties on Aerial Distribution," ASAE Paper No. AA91-003, NAAA/ASAE Technical Session, Las Vegas Nevada.

4. Brazelton, R.W., N.B. Akesson, and W.E. Yates. 1968. "Dry Materials Distribution by Aircraft," Transactions of ASAE, Vol. 11, No. 5, pp. 635-641.

5. Bouse, L.f. and J.B. Carlton. 1985. "Factors Affecting Distribution of Herbicides Pellets by Aircraft," Transactions of ASAE, Vol. 28(1), pp. 17-22.

6. Davis, J.B. and C.E. Rice. 1975. "Predicting Fertilizer Distribution by a Centrifugal Distributor Using CSMP- A Simulation Language," Transactions of ASAE, Vol.17, No. 6, pp. 1091-1093.

7. Gandrud, D.E., and Haugen, N.L. 1985. "Dry Application of Dry Flow-able Formulae," Pesticide Formulations and Application Systems - Fourth Symposium. T.M. Kaneko and L.D. Spicer Eds., American Society for Testing and Materials, Philadelphia, pp. 158-166.

8. Gardisser, D.R. 1992 . "Computer Simulation of Dry Material Distribution Patterns from Agricultural Aircraft," Ph.D. Thesis. University of Arkansas, Arkansas.

9. Griffis, C.L., D.W. Ritter, and E.J. Mathews. 1983. "Simulation of Rotary Spreader Distribution Patterns," Transactions of ASAE, Vol.26 No.1, pp. 33-37.

10. Hofstee, J.W. 1994. "Handling and Spreading of Fertilizers: Part 3, Measurement of Particle Velocities and Directions with Ultrasonic Transducers, Theory, Measurement System, and Experimental Arrangements," Journal of Agricultural engineering Research, Vol. 58, pp. 1-16.

11. Kennedy, J.B. and A. M. Neville. 1986. " Basic Statistical Methods for Engineers and Scientists," 3ed., Harper and Ron Publishers.

12. Law, S.E. and J.A. Collier. 1973. "Aerodynamic Resistance Coefficients of Agricultural Particulates Determined by Elutriation," Transaction of ASAE, Vol. 16, No. 5, pp. 918-921.

13. Lee, K.C. and W.E. Yates. 1977. "A Rotary Cylinder Spreader for Aircraft Granular Applications," Transactions of ASAE, Vol. 20 No. 5, pp. 801-805.

Limited, Longman House, Burnt Mill, Harlow Essex, UK

14. Morsi, S. A., A. J. Alexander. 1972. "An Investigation of Particle Trajectories in Two-phase flow System ," Journal of Fluid Mechanics, Vol. 55, part 2, pp. 193-208.

15. Olieslagers, S. H. Ramon, and J.De Baerdemaker. 1996. "Calculation of fertilizer distribution Patterns from a Spinning Disc Spreader by means of a Simulation Model," Journal of Agricultural engineering Research, Vol 63, pp. 137-152.

16. Pitt, R. E., G.S. Farmer, and L.P. Walker, 1982. " Approximating Equations for Rotary Distributor Spread Patterns" Transactions of ASAE, Vol. 25 No.6, pp. 1544-1552.

17. Reed, W.B., and Wacker, E. 1970. "Determining Distribution Pattern of Dry Fertilizer Application," Transactions of ASAE, Vol.13, No. 1, pp. 85-89.

18. Reints, R.E., and R.R.Yoerger. 1967. "Trajectories of Seeds and Granular Fertilizers," Transactions of ASAE, Vol. 10, No. 2, pp. 213-216.

19. Ritter, D.W., C. L. Griffis, and E. J. Mathews. 1980.Computer Simulation of Rotary Spreader Simulation Patterns. ASAE Paper No. 80-1504. ASAE, St. Joseph MI 49085.

20. Rosenberg, N.J. 1984. "Micro-Climate - The Biological Environment," 2ed., Chapter 4, pp. 100-105.

21. Roth, L.O., R.W. Whitney, and D.K. Kuhlman. 1985. "Application Uniformity and some Non-Symmetrical Distribution Patterns of Agricultural Chemicals," Transactions of The ASAE, Vol. 28, No. 1. pp.47-50.

22. Saunders, C. and W. B. Barr, 1992. "Uniform Patterns of Deposit of Vectobac by a Helicopter Flown Simplex Aerial Seeder After Adjustments and Modifications to the Aerial Seeder," Unpublished report, Parks and Recreation, City of Edmonton.

23. Spugnoli, M. Vieri and M. Zoli. 1989. "Testing of Spreaders for Granular Fertilizer," Land and Water Use, Dodd and Grace (eds.), Balkema, Rotterdam. pp. 2175-2179.

24. Teske, E.M., James, F. B., James, E. R. 1993. "FSCBG: An Aerial Spray Dispersion Model for Predicting the Fate of Released Material Behind Aircraft," Environmental Toxicology and Chemistry, Vol. 12, pp. 453-464.

25. Whitney, R.W., L.O. Roth, and D.K. Kuhlman. 1987. "Deposition Uniformity of Aerially Applied Granules," Transactions of ASAE, Vol. 30, No. 2, pp.332-337.

26. Winoto,S.H., 1990. "A Prediction Method for Particles Trajectories in Two-Phase Flow Systems," The International Journal of Storing, Handling, and processing Powder. Vol.2, No. 4, pp. 311-313.

27. Wirth, K. E. and O. Molerus. 1985. "Critical Solids Transport Velocity with Horizontal Pneumatic Conveying, "Journal of Powder and Bulk Soloids Technology, Vol. 9, No. 1, pp. 17-24.

28. Yates, W.E., J. Stephenson, K.Lee, and N.B. Akesson. 1973. "Dispersal of Granular Materials from Agricultural Aircraft," Transactions of ASAE, Vol. 16, No. 2, pp. 609-614.